

~~CONFIDENTIAL~~

TECH LIBRARY KAFB, NM
0143589

~~CONFIDENTIAL~~
NACA

RESEARCH MEMORANDUM

INTERNAL-FILM COOLING OF ROCKET NOZZLES

By J. L. Sloop and George R. Kinney

Flight Propulsion Research Laboratory
Cleveland, Ohio

CLASSIFIED (or changed to Unclassified)
BY: NASA Tech Rep Announcement #18
(OFFICER AUTHORIZED TO CHANGE)

By 27 Feb 52

JK
(GRADE OF OFFICER MAKING CHANGE)

12 Apr 61
DATE

CLASSIFIED DOCUMENT

~~CONFIDENTIAL~~
This document contains classified information
National Defense of the United
States, as defined by the Espionage Act,
USC, 18 USC, 793 and 794. The transmission or the
revelation of its contents in any manner to an
unauthorized person is prohibited by law.
Information so classified may be imparted
only to persons in the military and naval
services of the United States, or to appropriate
civilian officers and employees of the Federal
Government who have a legitimate interest
therein, and to United States citizens who are
loyally and discretion who of necessity are
informed thereof.



**NATIONAL ADVISORY COMMITTEE
FOR AERONAUTICS**

WASHINGTON

June 8, 1948

4-9-48/12



NATIONAL ADVISORY COMMITTEE FOR AERONAUTICS

RESEARCH MEMORANDUM

INTERNAL-FILM COOLING OF ROCKET NOZZLES

By J. L. Sloop and George R. Kinney

SUMMARY

Experiments were conducted to determine the feasibility of cooling a convergent-divergent rocket nozzle by the introduction of a coolant along the inside surface of the nozzle entrance (internal film cooling). Modifications were made to a 1000-pound-thrust engine using red fuming nitric acid and aniline as propellants. Water was introduced as a coolant by two methods: (1) an arrangement of 36 individual jets directed in a fanlike pattern downstream along the nozzle wall, and (2) the use of a porous-metal ring located at the nozzle entrance. Effectiveness of cooling was determined by the average heat-absorption rate of a massive copper nozzle and by wall temperatures along the outside surface of a thin-wall nozzle of low heat capacity.

Experiments with uncooled nozzles showed that the maximum wall temperature occurred in the convergent section near the throat. The nozzle-cooling investigations were limited but showed that film cooling with water, when introduced by either of the methods used at a rate of 3 percent of the propellant flow, reduced the heat flow into the nozzle to about 55 percent of the heat flow for uncooled conditions. Introduction of the water through the porous metal ring resulted in a more uniform distribution of the coolant than the use of the jets directed along the nozzle wall. Wall temperatures in the throat and divergent sections of the nozzle were not stabilized by cooling for the conditions used. Film cooling with water reduced the specific impulse (with the weight of water included) about in the same ratio as the ratio of water consumption to propellant consumption.

INTRODUCTION

In a rocket engine, all the working fluid can be oxidant and fuel; a large amount of energy can thus be liberated in a small volume. These large rates of release of energy, which produce gas temperatures from 3500° to 6500° F or higher, create a severe cooling problem; in some cases, engine performance can be seriously limited by the necessity for cooling. For rocket engines involving such

propellant combinations as red fuming nitric acid plus aniline and liquid oxygen plus hydrocarbon fuel, typical heat-transfer values in the combustion chamber and in the nozzle throat are 1 and 4 Btu per second per square inch, respectively. For high-energy propellant combinations, such as those involving fluorine and liquid oxygen as oxidants and hydrazine, hydrogen, boron compounds, and metal compounds as fuels, the heat-transfer rates are probably much greater than the values cited.

In spite of large heat-transfer rates, rocket engines can be successfully operated without cooling for short periods of time. For long periods of operation, some rocket engines have been regeneratively cooled with one or both propellants flowing over the outer surfaces of the combustion chamber and nozzle prior to injection into the combustion chamber. Regenerative cooling, however, is contingent on the ability of the propellant-coolant fluid to absorb all the heat flow into the engine walls and still satisfactorily function in the injection and mixture processes. For many rocket engines, the propellants used have insufficient heat capacity to absorb the heat flow or the propellants are thermally so unstable that their use as coolants is restricted or impossible. For such cases, a promising cooling method is internal-film or boundary-layer cooling whereby the temperature of the engine walls is maintained at a safe value by a coolant film on the inner surface. The coolant may be either a propellant or a separate fluid and may be introduced as a liquid or as a gas. The internal cooling film may be established in a variety of ways that includes, for example, the use of holes through the inner engine wall, injectors for directed jets or sprays, annular openings, and areas of wire cloth, porous metal, or porous ceramic through which the coolant may be introduced. The best-known example of regenerative and film cooling is the engine of the German A-4 rocket missile (V-2), which used the fuel (75-percent ethyl alcohol and 25-percent water) as the coolant.

Porous metals for rocket-engine-cooling applications have gained widespread interest because of the possibilities of a method known as transpiration cooling and of internal-film cooling. In transpiration cooling, the entire surface is made porous and just enough coolant is forced through the metal so as to keep the temperature of the porous metal at a safe value. If a liquid coolant is used, the flow rates must be greater than the cooling requirements for the porous metal to avoid the possibility of vaporization within the porous metal. This condition results in uncontrollable overheating. The use of a gaseous coolant avoids vaporization difficulties and permits a high operating temperature of the porous wall. In internal-film cooling, either porous-metal rings or segments can be used to establish the film that provides thermal insulation of the wall for some distance downstream of the point of introduction. In this

application, a liquid coolant can be advantageously used because the coolant flow is much greater than that needed to cool the porous surfaces alone. Much work on porous metals for rocket cooling has been done by the Jet Propulsion Laboratory of the California Institute of Technology.

The nozzle of the rocket engine presents the most severe cooling problem of the engine because the accelerated gas flow through the nozzle greatly increases the heat transfer by forced convection; in the nozzle throat, for example, the heat flow is several times greater than that in the combustion chamber. An investigation was made at the Jet Propulsion Laboratory of the California Institute of Technology of film cooling of a rocket combustion chamber and nozzle by holes in the inner wall in a manner similar to the engine of the German A-4 rocket missile, but in the experiments the cooling effects in the combustion chamber and the nozzle were not separated.

An experimental program was initiated at the NACA Cleveland laboratory in order to determine the effect of various rates of coolant flow introduced at the nozzle entrance on the heat transfer to the nozzle, on nozzle temperature distribution, and on the specific impulse of the rocket engine. These experiments, reported herein, were limited to the use of water as a coolant and to two methods of establishing the internal film: (1) an arrangement of 36 small jets directed in a fanlike pattern downstream along the nozzle walls, and (2) passage of the coolant through a porous-metal ring. The cooling effectiveness was determined by measuring the average heat-absorption rate of a massive copper nozzle and by measuring outer-wall temperatures at a number of positions on a thin-wall nozzle of low heat capacity. Result of preliminary experiments with an engine completely cooled by liquid films are described in the appendix.

APPARATUS AND PROCEDURE

Engine installation. - Tanks and control equipment from an assisted take-off unit (25-ALD-1000) were used for the experiments. A schematic flow diagram of the propellant and coolant supply system is shown in figure 1 for the experimental 1000-pound-thrust engine used for the experiments. The standard control system of the take-off unit was modified to allow pressurization of the propellant tanks before operation of the propellant flow valves; full flow could therefore be rapidly established when the propellant flow valves were opened. For some of the runs, the restrictor check valve in the nitrogen supply line to the acid and the aniline flow valves was removed for rapid operation of the valves. The engine and propellant-tank assembly was suspended and stabilized by guy wires that permitted motion in the direction of engine thrust.

Propellants and coolant. - The propellants used were aniline and red fuming nitric acid. The acid contained a minimum of 6-percent excess nitrogen dioxide by weight in solution and a maximum of 5-percent water by weight. The propellants were chosen because of availability and convenience as a source of hot gases and not because of specific cooling problems involving these propellants. Water was chosen as a coolant because of convenience and known properties.

Engine assemblies. - Diagrammatic sketches of parts of the rocket engine and the various cooling systems used for the nozzle-cooling experiments are shown in figure 2. The injector plate, the combustion chamber, and the massive chrome-plated copper nozzle are from a type 25-AL-1000 assisted take-off unit. The injector plate provided for four pairs of impinging jets; for the design acid-aniline ratio of 1.5, the resultant direction of the impinging jets was approximately axial. For the nozzle-cooling experiments, however, the acid-aniline ratio was 3 and for this ratio the resultant direction of the impinging jets was about 90° inward. The combustion chamber was thermally insulated by asbestos gaskets from the cooling sections and operated uncooled. The copper nozzle, insulated from the cooling sections by mica and asbestos gaskets, was used to obtain average heat-absorption rates. Thermocouples were embedded in the copper nozzle at several positions to obtain the temperature rise of the copper mass. The thin-wall stainless-steel nozzle was used for heat-distribution surveys. A sketch of this nozzle and the location of 22 thermocouples welded to the outer surface in order to obtain wall temperatures in axial and circumferential directions is presented in figure 3. Ten of the thermocouples lie in the same plane along the nozzle contour. In addition, three thermocouples spaced 90° apart were located at each of stations 1, 3, 5, and 9. A photograph of the thin-wall stainless-steel nozzle with part of the thermocouple installation is shown in figure 4.

The equipment used to establish internal films and control-run equipment is also shown in figure 2. Section A was a chrome-plated copper ring used for uncooled control runs. Section B was a steel ring containing 12 equally spaced stainless-steel injectors and a second steel ring used as a spacer to make the length of section B the same as for other sections. The injectors projected about $1/8$ inch into the combustion chamber and each contained three 0.0135-inch diameter holes for directing jets of water downstream in a fanlike pattern along the nozzle wall as indicated. A photograph of this injector ring is shown in figure 5. Section C (fig. 2) was a porous bronze ring 1.5 inches long and encased in an aluminum housing. Distilled water was forced inward through the porous ring and was carried downstream through the nozzle by the flowing gases. Two porous-wall sections were used and differed from each other only

in the ring thickness and thermocouple installation. The first ring was 1/2 inch thick and had nine chromel-alumel thermocouples spaced around the circumference with the junctions located near the inner surface of the ring. A tenth thermocouple was installed in the annular water feed to the porous ring. A photograph of the porous ring in the aluminum housing with the thermocouples installed is shown in figure 6. The second ring was 1/4 inch thick and five copper-constantan thermocouples were installed around the circumference. One thermocouple was embedded in the porous metal near the inner surface, one was embedded near the outer surface, and three were installed flush with the inner surface and thermally insulated from the porous metal. Section D (fig. 2) provided for two jets radially directed inward that carried the water away from the wall in order to compare this method with the methods in which the water was directed along the wall.

Measurements. - Thrust was measured by a bar spring equipped with two wire strain gages connected in a resistance bridge circuit. A modified, self-balancing, recording potentiometer plotted the variation of thrust with time. The entire system was calibrated by applying dead-weight forces in the same direction as engine thrust. Two thrust-measuring bars were used. For one bar, four calibrations over a period of 2 weeks agreed within 0.6 percent at an applied force of 1000 pounds. Similar calibrations with the second bar over a period of 6 months gave results that agreed within 1.2 percent for all calibrations. Propellant and coolant consumptions were determined by placing weighed quantities of the fluids in the tanks before the run and by weighing the amount of fluid drained from the tanks after the run. Engine operation was always stopped before exhaustion of any of the fluids. Combustion-chamber pressure was measured by a Bourdon pressure recorder. Temperatures were obtained by chromel-alumel and copper-constantan thermocouples and by three types of recorder: (1) self-balancing potentiometers, (2) photoelectric microammeters, and (3) a multichannel oscillograph.

Specific impulse was computed by integrating the thrust-time record by a planimeter and dividing by the sum of the propellant and coolant consumptions. For the runs in which specific impulse was determined, the accuracy of this measurement was increased by provision for rapid opening and shutting of the acid and the aniline flow valves. This provision gave more constant flows and rapid development and cut-off of full engine thrust. The heat absorbed by the copper nozzle was computed as the product of temperature rise, specific heat of copper at the average nozzle temperature, and nozzle weight. The runs varied in time from 10 to 19 seconds and temperatures throughout the copper nozzle were equalized about 60 seconds after start of combustion. This temperature was used to calculate the heat

stored in the nozzle at that time. From measurements of the rate of heat loss during several minutes after the end of combustion, a correction factor for heat loss to the surrounding atmosphere was determined. This correction factor was used to estimate the heat loss during the 60-second period. The heat loss amounted to between 3 and 10 percent of the heat absorbed by the nozzle during combustion and was added to the heat stored in the nozzle, which was determined from the equilibrium temperature.

Operating conditions. - The operating conditions for the nozzle-cooling experiments were:

Thrust, lb	1050±50
Chamber pressure, lb/sq in. absolute	290±10
Combustion time, sec	.1 to .19
Oxidant-fuel ratio	3.0±0.2
Propellant flow, lb/sec	6.1±0.3
Coolant flow, percent of propellant flow	0 to 9

RESULTS AND DISCUSSION

Copper-nozzle experiments. - The average nozzle heat-absorption rate and specific impulse are shown in figure 7 for four types of run: (1) uncooled (reference condition), (2) with water-jet cooling directed along the nozzle wall, (3) with cooling by water seeping through a porous wall before the nozzle, and (4) with water injection away from the wall before the nozzle (reference condition). For the uncooled runs, the average nozzle heat-absorption rate was 1.49 ± 0.05 Btu per second per square inch. The runs with cooling show some scatter, part of which is attributed to uncertainties in the measurement of water flow. At a water flow of 3 percent of the propellant flow, the nozzle heat-absorption rate was about 55 percent of the rate for the uncooled runs. Only two runs were made with the porous ring (1/2 in. thick), one at 2.3 and the other at 3.2 percent of the propellant flow; the results fell along the same curve (fig. 7) as those for the injection with water jets directed along the nozzle wall. For water flows from 4 to 8 percent of the propellant flow with water jets directed along the nozzle wall, the nozzle heat-absorption rate showed no appreciable change. The high nozzle heat-absorption rates for the runs where water was introduced away from the wall clearly show that the observed reductions in nozzle heat-absorption rates for water introduced along the wall were caused by cooling of the boundary layer. Heat-transfer rates and engine performance were slightly higher for these two control runs than for uncooled runs because the propellant flow was about 8 percent higher. The higher propellant flow was caused by a higher injection pressure.

The specific impulses obtained during the cooling experiments are also shown in figure 7. The specific impulse for the runs without cooling was 177.3 pound-seconds per pound and this value is about 80 percent of the theoretical performance. For a water flow of 3 percent of the propellant flow, the specific impulse with the weight of water included was reduced about 3 percent from that for uncooled operation.

For the run with the porous ring and a water flow of 3.2 percent of the propellant flow, the water temperature measured in the water supply annulus for the porous ring rose from 39° to 62° F during 15 seconds of operation and the maximum temperature for thermocouples in the porous metal was 68° F. For the run with a water flow of 2.3 percent of the propellant flow, the water in the annulus rose from 55° to 81° F in 9 seconds and porous-metal temperatures at six circumferential positions on the surface of the porous metal were 86°, 98°, 135°, 155°, 174°, and 305° F. This wide variation in porous-metal temperature indicates a nonuniform coolant flow through the ring, which was caused by accidental overheating and carbon fouling of the porous ring during a preliminary run at a low coolant flow. For all experiments with porous-metal rings, difficulty was experienced with plugging of the porous metal. Deposits of carbon always appeared on the porous surface even when an excess of water was continuously pumped through the ring before, during, and after combustion. This difficulty could be avoided by the use of propellants containing only oxygen, hydrogen, and nitrogen. The progressive plugging appeared to be of a permanent nature and in addition to the carbonaceous deposits, the plugging may also have been caused by contaminants in the distilled water (in spite of elaborate precautions), gas entrapment, and hydraulic damage to the internal pore structure of the porous bronze.

Some of the small-diameter holes (0.0135 in.) of the water injectors (fig. 2, section B) were clogged with carbonaceous deposits after a run and had to be cleaned and checked after each operation. In addition, small water jets were difficult to direct in a desired manner because critical manufacturing tolerances were required. Difficulties of this nature would probably not be encountered if larger jets in larger engines were used.

Thin-wall nozzle experiments. - The length of three uncooled runs with the thin-wall nozzle was necessarily short because of the low heat storage capacity, and varied from 0.8 second for the first run to slightly over 2.4 seconds for the second and third runs; these two times were chosen for wall-temperature comparisons between uncooled and cooled runs. The wall temperatures at a number of positions for an uncooled run at the selected times of 0.8 and 2.4 seconds are shown

in figure 8. The curves show a maximum wall temperature in the convergent section at station 3 (fig. 3), which is approximately 1 inch upstream of the nozzle throat. Some circumferential temperature variation occurred especially in the convergent section. Wall temperatures along a contour line oriented at the 3 o'clock position looking upstream were higher in most cases than other circumferential points at the same upstream distance; this tendency was also observed for the other uncooled runs. Some insight of the variation of the initial heat-transfer rate with axial position in the nozzle can be obtained from inspection of the curves of wall-temperature variation with axial position. For this purpose, the curve at 0.8 second is better than the curve at 2.4 seconds.

The reproducibility of the wall temperatures at 0.8 second and at 2.4 seconds for the three uncooled runs is shown at several positions by the following table:

Run	Time (sec)	Temperature (°F)							
		Convergent section			Throat	Divergent section			
		Station			Station	Station			
		2	3	4	5	7	8	9	10
1	0.8	419	554	285	451	294	158	276	181
2	.8	326	537	438	408	312	176	306	201
3	.8	400	643	472	399	266	149	300	172
Maximum difference		93	106	187	52	46	27	30	29
2	2.4	1087	1320	918	1351	840	480	594	431
3	2.4	1291	1574	1112	1397	840	480	602	450
Maximum difference		204	254	194	46	0	0	8	19

Wall temperatures at all stations except station 5 (throat) are for the vertical position. The throat wall temperature was at the 3 o'clock position looking upstream. At runs for both 0.8 and 2.4 seconds, the wall temperatures for any position in the throat and the divergent sections agreed more closely than the wall temperatures at any position in the convergent section. Temperature variations in the convergent section, as observed for comparable runs in this investigation, introduce an additional complication in the problem of cooling the convergent section.

The results of cooling the thin-wall nozzle by a water flow of 3.5 percent of the propellant flow passing through a 1/4 inch thick porous ring before the nozzle are shown in figure 9. The wall temperatures for the uncooled run (fig. 8) are replotted for comparison. The wall temperatures at 0.8 second are shown in

figure 9(a); at this time, the effect of cooling is clearly apparent in the convergent section and in the throat; whereas there is no appreciable cooling effect in most of the divergent section. The wall temperatures at 2.4 seconds are shown in figure 9(b). The effect of cooling in the convergent section is still apparent but the throat temperatures have risen considerably and the temperatures in the divergent section are near the values for the uncooled run. The maximum wall temperature measured for the cooled run at 2.4 seconds was 820° F and this temperature occurred at a position in the throat. The wall temperature at this point continued to rise and became so high after 9 seconds (fig. 9(c)) of operation that the run was stopped. With one exception the wall temperatures in the convergent section after 9 seconds remained comparatively low, between 300° and 410° F. The one exception was adjacent to the hot spot at the throat. Two wall temperatures at the throat were 1390° and 1944° F and the wall temperatures in the divergent section ranged from 1035° to 1424° F. These high temperatures in the throat and divergent sections indicate inadequate cooling for the conditions used. No data for the corresponding uncooled run for 9 seconds are shown in figure 9(c) because without cooling the nozzle burned out in 4 seconds.

A plot of wall temperature as a function of time is presented in figure 10 for several of the positions shown by figure 9. A wall temperature at station 1 (the station nearest to the porous ring) is shown in figure 10(a) and is representative of the four wall temperatures recorded at this station for the cooled run. The stabilizing effect of the water film on the wall temperature is clearly apparent. Temperatures at three circumferential positions at station 3 in the convergent section where the maximum wall temperatures for uncooled runs occurred are shown in figure 10(b). The wall temperatures for the uncooled run rose rapidly but for the cooled run two wall temperatures stabilized at about 400° F. The third wall temperature followed the other two for about 4 seconds after which time it began to increase rapidly. As previously mentioned, this rapid rise of temperature is probably caused by the presence of an adjacent hot spot in the throat. The variation of wall temperatures at two circumferential positions at station 5 at the throat are shown in figure 10(c). Although both wall temperatures rose more slowly during the cooled run than the uncooled run, the cooling was inadequate to stabilize the wall temperature at a safe working temperature. The variation of wall temperature in the divergent section near the exit is shown in figure 10(d). The data, typical of all data recorded for the divergent section, show a rapid rise of wall temperature for both uncooled and cooled runs. Although the cooling effect in the divergent section is discernable, it was inadequate for steady-state cooling of the divergent section for the operating conditions used.

The temperature at the outer surface of the porous ring rose from 64° to 82° F in 9 seconds of operation and the temperature at a position near the inner surface of the porous metal rose to 89° F. Three thermocouples exposed to the combustion chamber indicated temperatures of 108° and 125° F at the top of the ring and 190° F at the bottom of the ring.

Wall temperatures of the thin-wall nozzle at several positions after 9 seconds of operation with water cooling by the jets directed along the nozzle wall at the entrance are shown in figure 11. The water flow was about 8.5 percent of the propellant flow. The results show the same trends as those with porous-ring cooling; that is, considerable cooling in the convergent section and ineffective cooling in the throat and divergent sections. The run with the directed jets was stopped after 10 seconds by the appearance of a hot spot in the throat region. A visual examination of the thin-wall nozzle after the run clearly indicated, by metal discoloration streaks, a nonuniform coolant coverage of the inner surface of the convergent section. The throat and divergent sections showed a uniform metal discoloration and hence no visible indication of nonuniformity in coolant coverage. A photograph of the thin-wall nozzle after this run is shown by figure 12 and the metal-discoloration streaks in the convergent section can be seen. These results indicate that the jets did not give as uniform a coolant coverage in the convergent section as did the porous ring; the nonuniformity of coolant coverage by jets may be caused by the particular jet pattern used. A different jet pattern where all the jets are directed at an angle to the gas flow to produce a helical path may be a better arrangement for uniform nozzle coverage, but this possibility was not investigated.

The results of the thin-wall nozzle experiments on nozzle cooling do not show steady-state cooling of the entire nozzle but indicate the possibility of cooling the convergent section by a reasonable amount of coolant introduced uniformly at the entrance of the nozzle. Additional cooling is required at the throat and in the divergent section. Further experiments are required to determine the most reliable methods of internal-film cooling.

SUMMARY OF RESULTS

Experiments on internal-film cooling a convergent-divergent nozzle were conducted with a modified 1000-pound-thrust commercial rocket engine using red fuming nitric acid and aniline at an oxidant-fuel weight ratio of 3.0 and combustion-chamber pressure of about 290 pounds per square inch absolute, which resulted in an average specific impulse of 177 pound-seconds per pound. Water was introduced as a coolant at the

903
nozzle entrance by two methods: (1) a single arrangement of 36 jets directed in a fanlike pattern along the nozzle wall, and (2) by means of a porous-metal ring located at the nozzle entrance. Cooling effectiveness was determined by the average heat-absorption rate of a massive copper nozzle and by wall temperatures at many positions on a thin-wall nozzle of low heat capacity. The nozzle-cooling experiments gave the following results:

1. For uncooled runs, the maximum recorded wall temperature of the thin-wall nozzle occurred in the convergent section a short distance upstream of the nozzle throat. For comparable uncooled runs, the wall temperature variation in the convergent section of the thin-wall nozzle was greater than the wall temperature variation in the throat and divergent sections.

2. A water flow through the porous ring of 3.5 percent of the propellant flow introduced at the entrance to the convergent section of the nozzle stabilized the wall temperatures in the convergent section except for one point, but inadequately cooled the throat and divergent sections. The one unstabilized point in wall temperature in the convergent section apparently resulted from the growth of a hot spot in the throat.

3. A water flow of 3 percent of the propellant flow, when introduced by either the directed jets along the nozzle wall or by the porous ring, reduced the average heat-absorption rate of the copper nozzle to about 55 percent of the uncooled value.

4. Increasing the water flows from 4 to 8 percent of the propellant flow with water jets directed along the nozzle wall caused no appreciable reduction in the heat-absorption rate of the nozzle.

5. A strict comparison between directed jets and porous-ring methods for film cooling was not made but the results indicate the porous ring gave a more uniform coverage of coolant in the convergent section and was more effective in cooling the convergent section of the nozzle than the particular water-jet arrangement used.

6. For film cooling with water, the specific impulse with the weight of water included was reduced in approximately the same ratio as the ratio of water consumption to propellant consumption.

Flight Propulsion Research Laboratory,
National Advisory Committee for Aeronautics,
Cleveland, Ohio.

APPENDIX - PRELIMINARY EXPERIMENTS WITH A FILM-COOLED ROCKET ENGINE

Prior to the experiments of nozzle-film cooling, a preliminary study was made on a one-piece combustion chamber and nozzle from the dropable assisted take-off unit previously described. The engine was modified as shown by figure 13 to include two rings of twelve coolant injectors in the combustion chamber at stations 1 and 2 and one ring of eight injectors in the convergent section of the nozzle at station 3. Each injector had three 0.0135-inch holes for directing water jets downstream in a fanlike pattern along the wall as shown. Chromel-alumel thermocouples were installed near the inner surface and were located behind each injector ring, in the throat, and in the nozzle exit.

No attempt was made to control accurately the operating conditions of the engine. From water calibrations, the acid-aniline ratio was 1.6. Thrust was approximately 1000 pounds and chamber pressure was about 265 pounds per square inch absolute. The propellant flow was about 6 pounds per second and the coolant flow was about 12.5 percent of the propellant flow.

The time-temperature variations during the run at each of the five thermocouple stations are shown in figure 14. Satisfactory agreement in wall temperatures at all positions was obtained for the two uncooled runs and at most of the stations for the cooled runs. For one uncooled run after 23 seconds of operation, the wall temperatures ranged from 660° F in the exit to a maximum of 1270° F in the convergent section of the nozzle (figs. 14(c) and 14(e)). The greater wall thickness at the throat is insufficient to account for the large temperature difference between the convergent section and the throat. The wall temperatures for one cooled run after 23 seconds of operation ranged from about 410° F in the combustion chamber to 620° F in the uncooled region behind the first ring of coolant injectors (figs. 14(a) and 14(b)). The differences of wall temperatures for the two cooled runs behind the first ring of coolant injectors (station 1) may be the result of one or more of the following conditions: (1) axial heat conduction along the 1/2 inch thick combustion chamber, (2) clogging of some of the water-jet holes near the thermocouples, and (3) backflow of coolant caused by propellant-injection turbulence and combustion fluctuations in that region. The wall temperatures behind the second and third coolant-injector rings (stations 2 and 3) are near stabilization before the end of the runs. The throat and exit wall temperatures were appreciably affected by the coolant but were not stabilized before the end of the runs.

These brief experiments did not result in steady-state cooling of the engine but they did serve as an indication of the range of magnitude of the variables involved and the practical problems encountered in using internal cooling by directed jets.

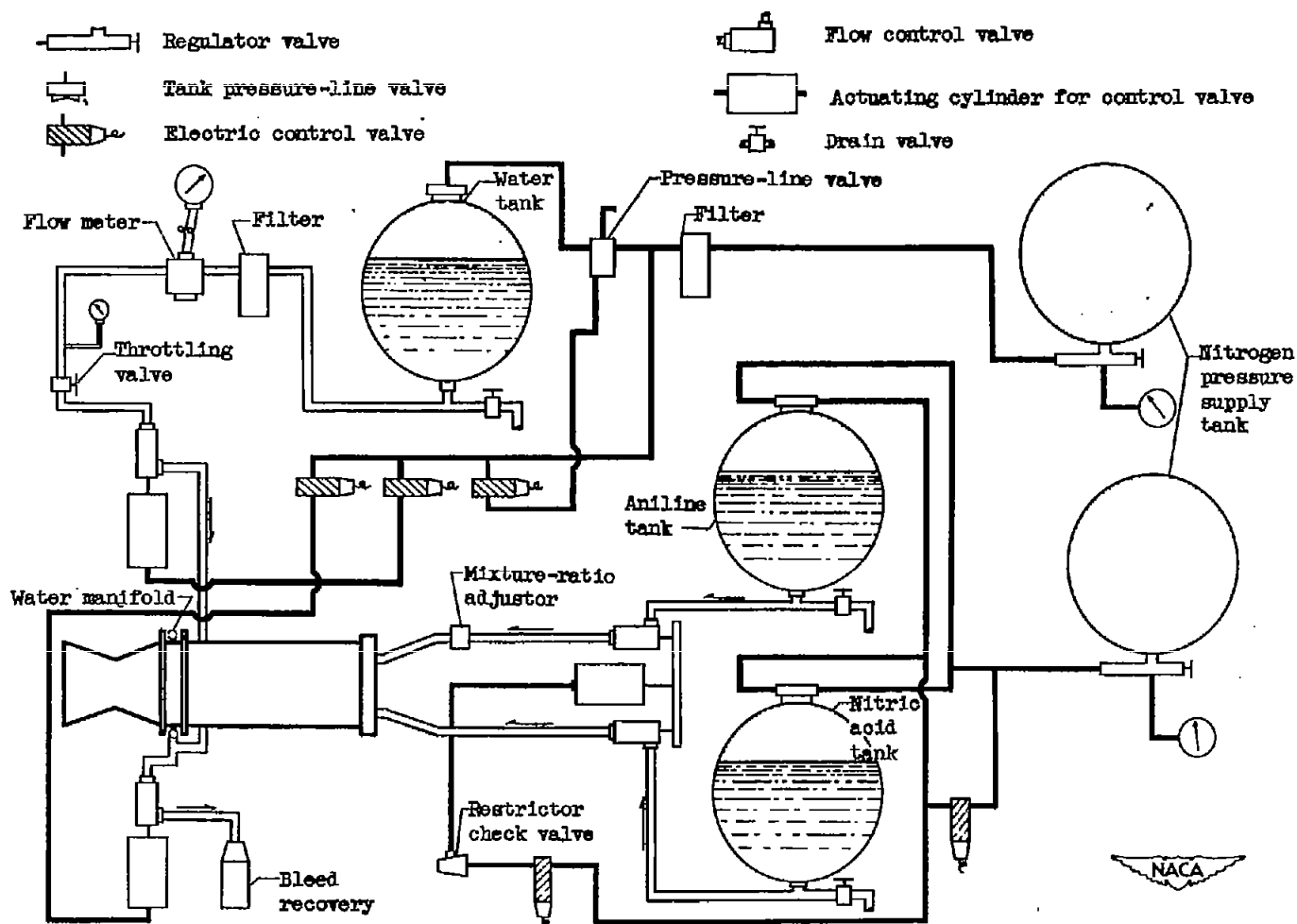


Figure 1. - Flow diagram of experimental 1000-pound thrust rocket engine using red fuming nitric acid and aniline as propellants and water as an internal coolant.

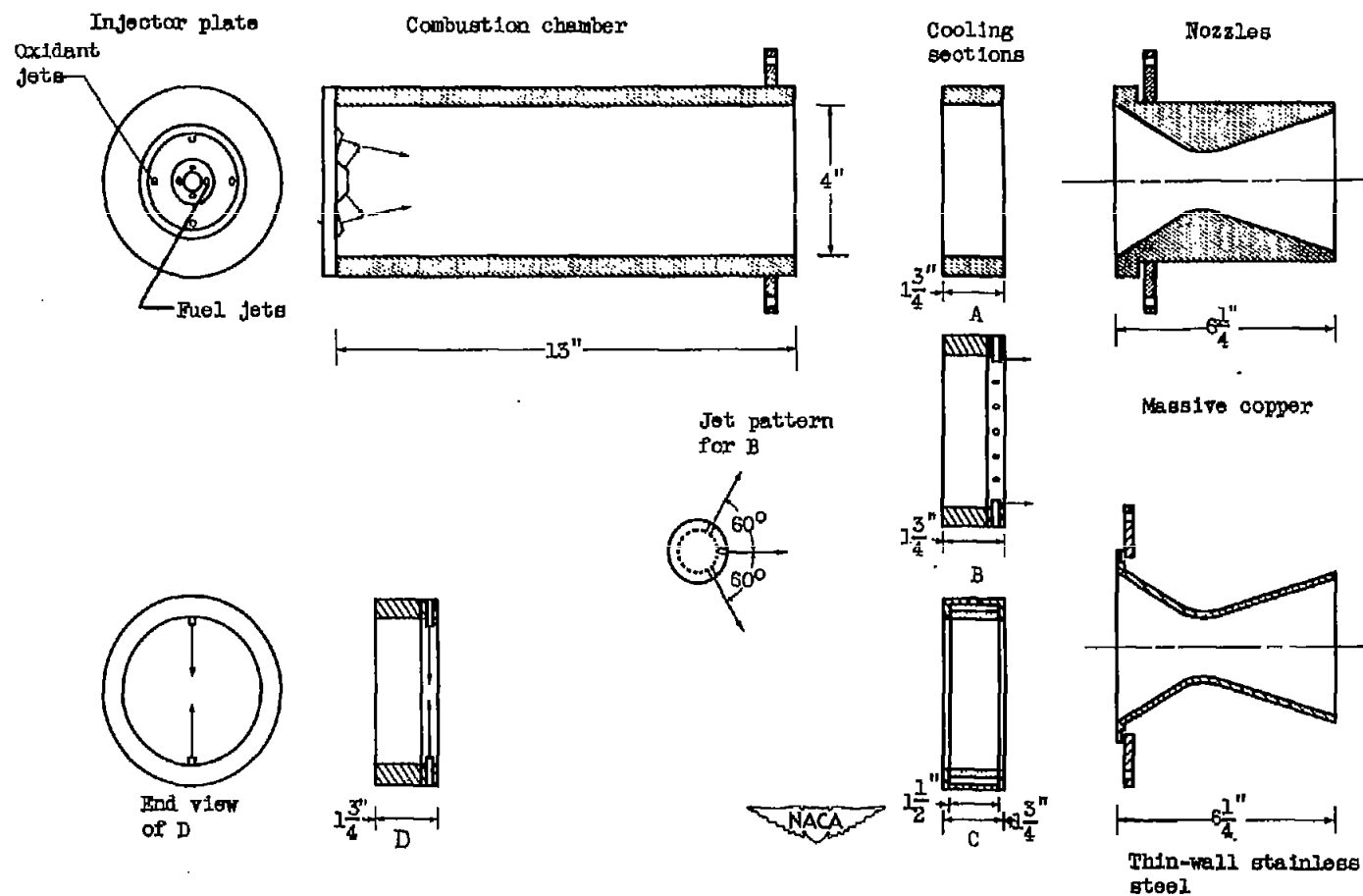


Figure 2. - Diagrammatic sketches of parts of rocket engine used in different combinations for nozzle-cooling experiments.

CONFIDENTIAL

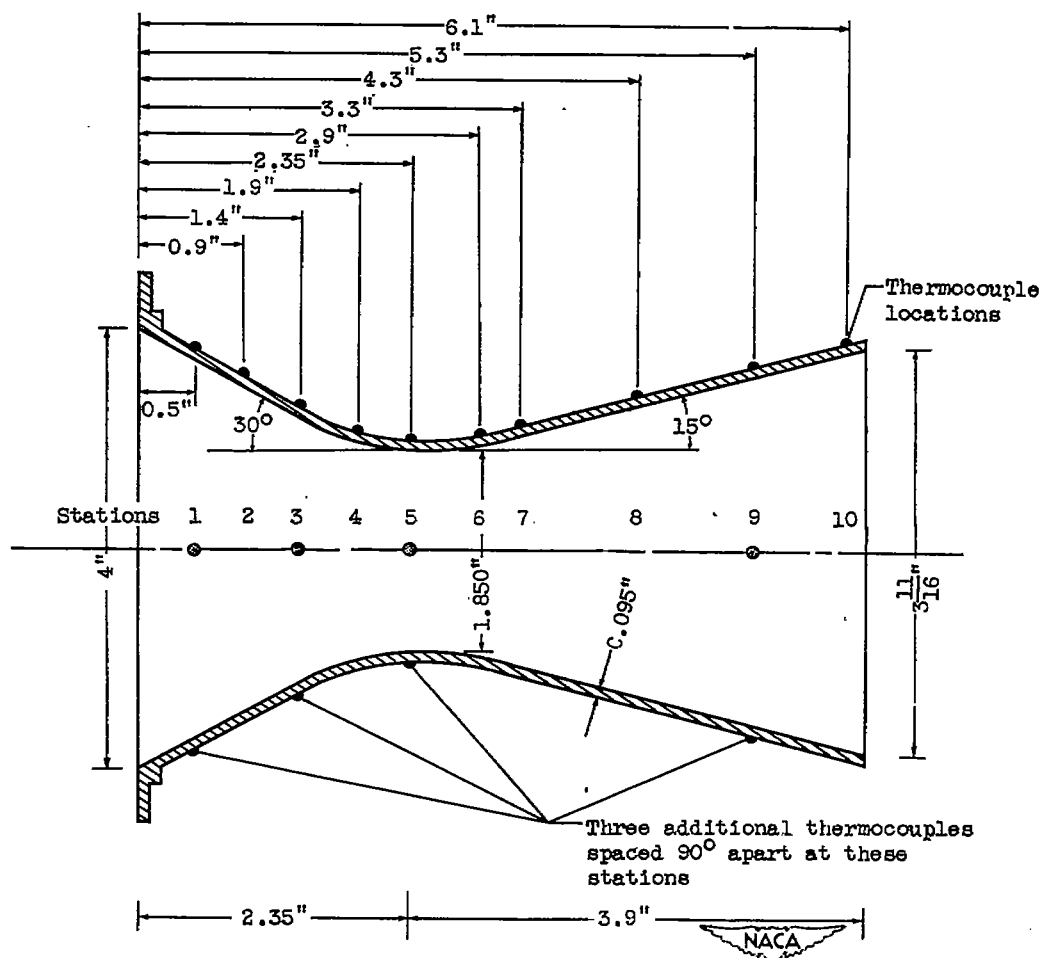


Figure 3. - Thin-wall stainless-steel nozzle showing location of ten thermocouples in straight line along nozzle contour and three additional circumferential thermocouples at each of stations 1, 3, 5, and 9.

CONFIDENTIAL

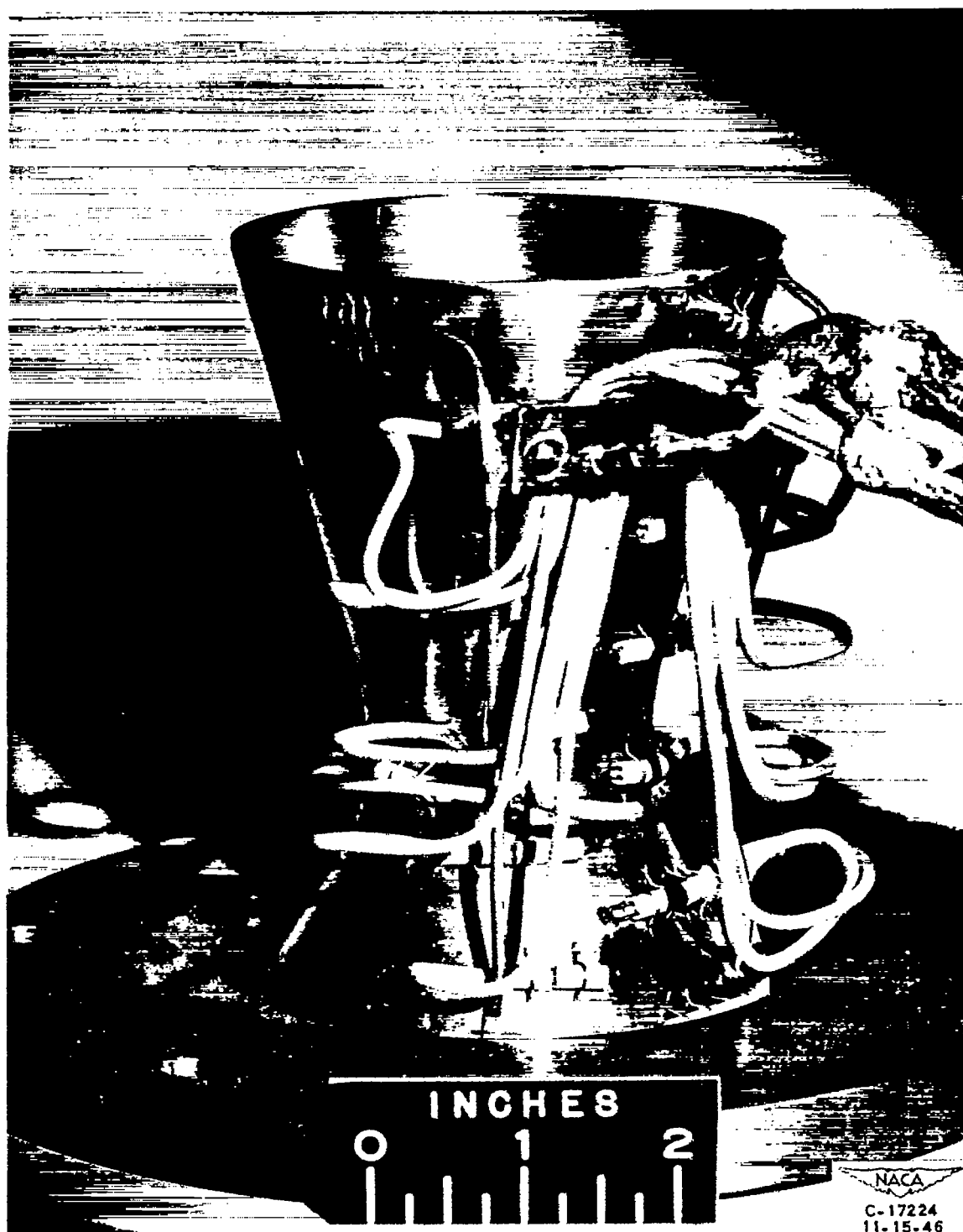


Figure 4. - Thin-wall stainless-steel nozzle showing part of thermocouple installation.

[REDACTED]

..

..

..

..

..

..

..

..

[REDACTED]

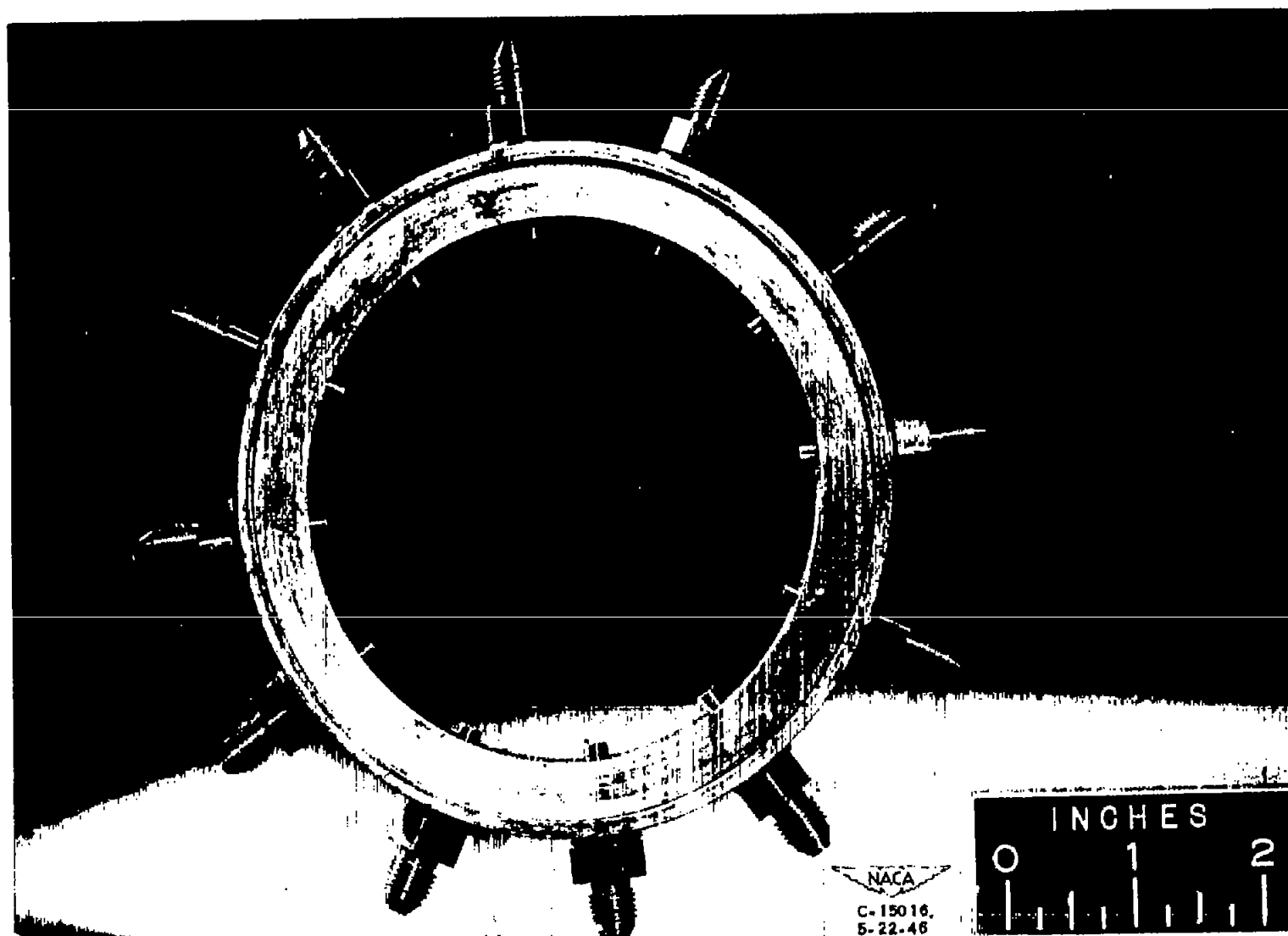


Figure 5. - Ring with twelve coolant injectors each with three directed jets.

[REDACTED]

[REDACTED]

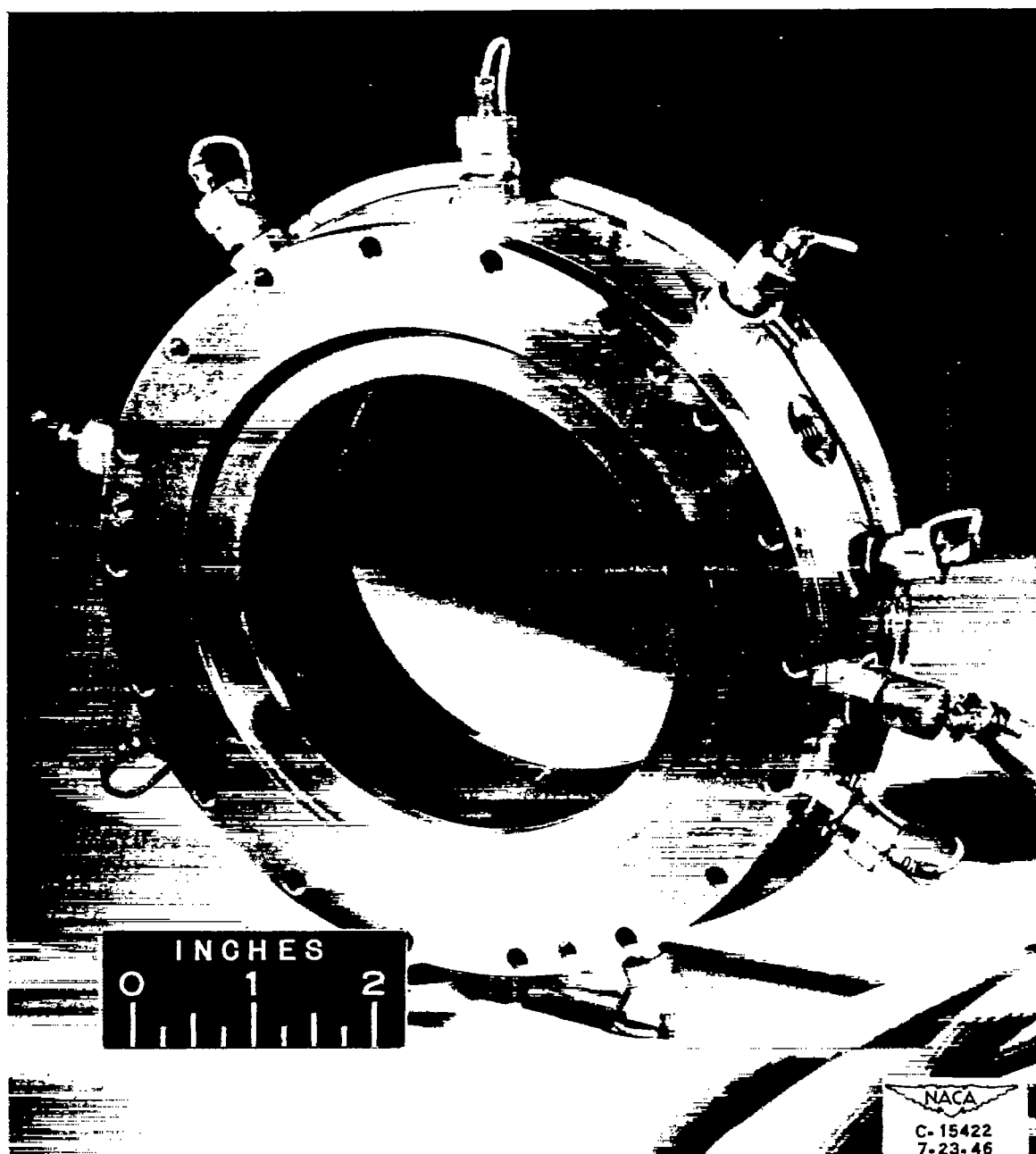


Figure 6. - Porous-metal ring and holder with thermocouples installed.

[REDACTED]

..

..

..

..

..

..

..

..

[REDACTED]

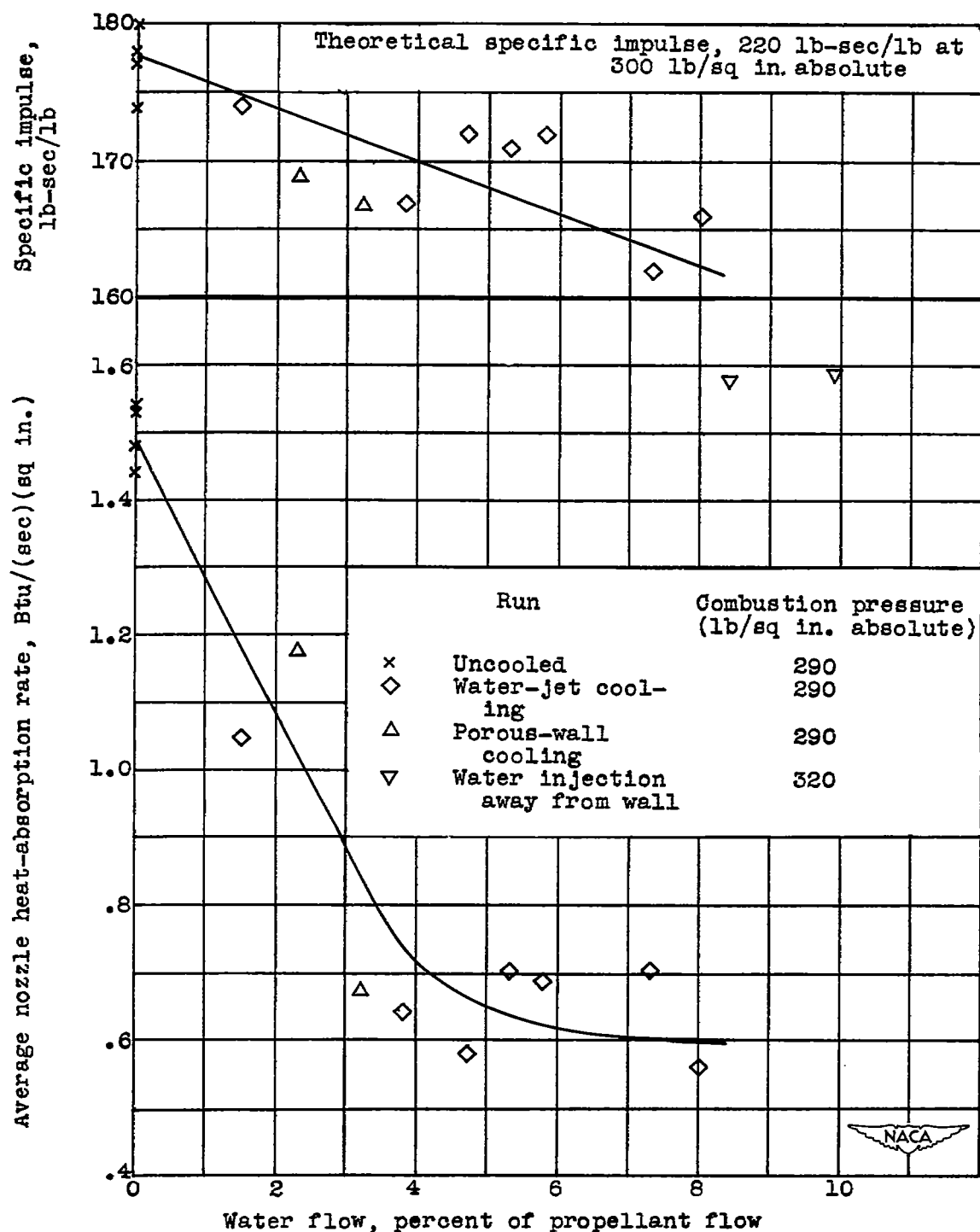


Figure 7. - Effect of internal-film cooling introduced at nozzle entrance on average nozzle heat absorption and on specific impulse of rocket engine.

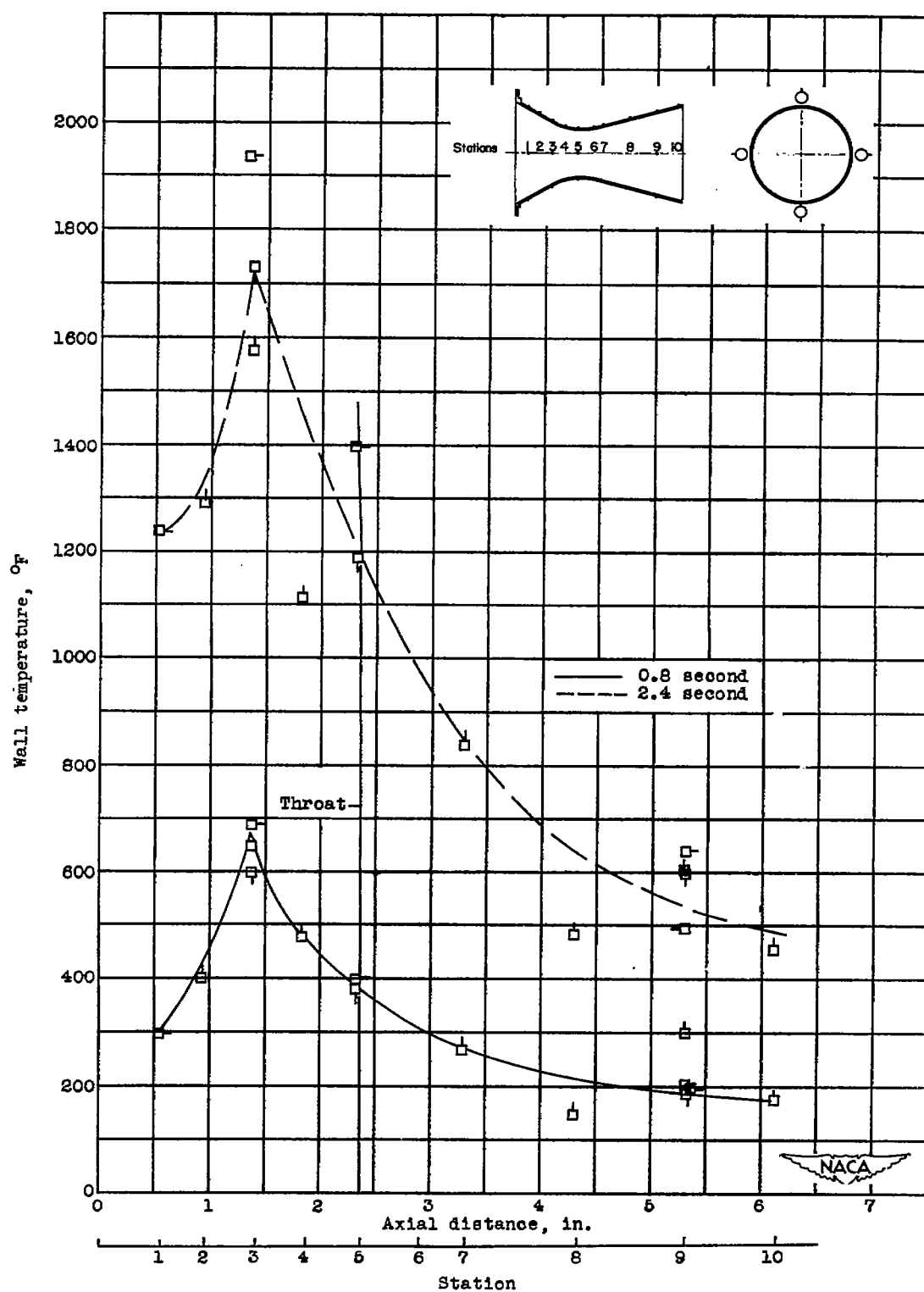


Figure 8. - Wall temperatures for uncooled thin-wall stainless-steel nozzle after 0.8 and 2.4 seconds.

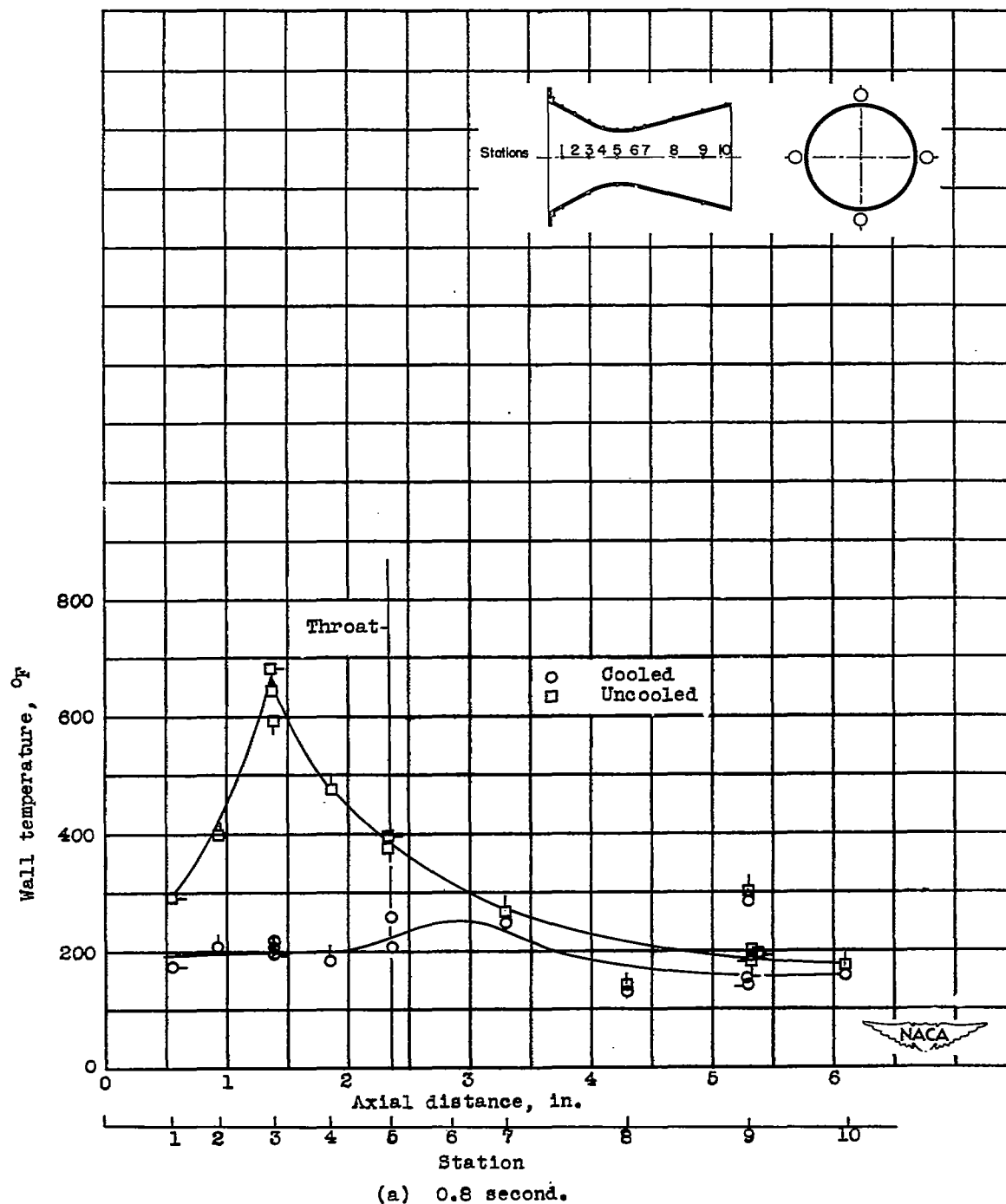
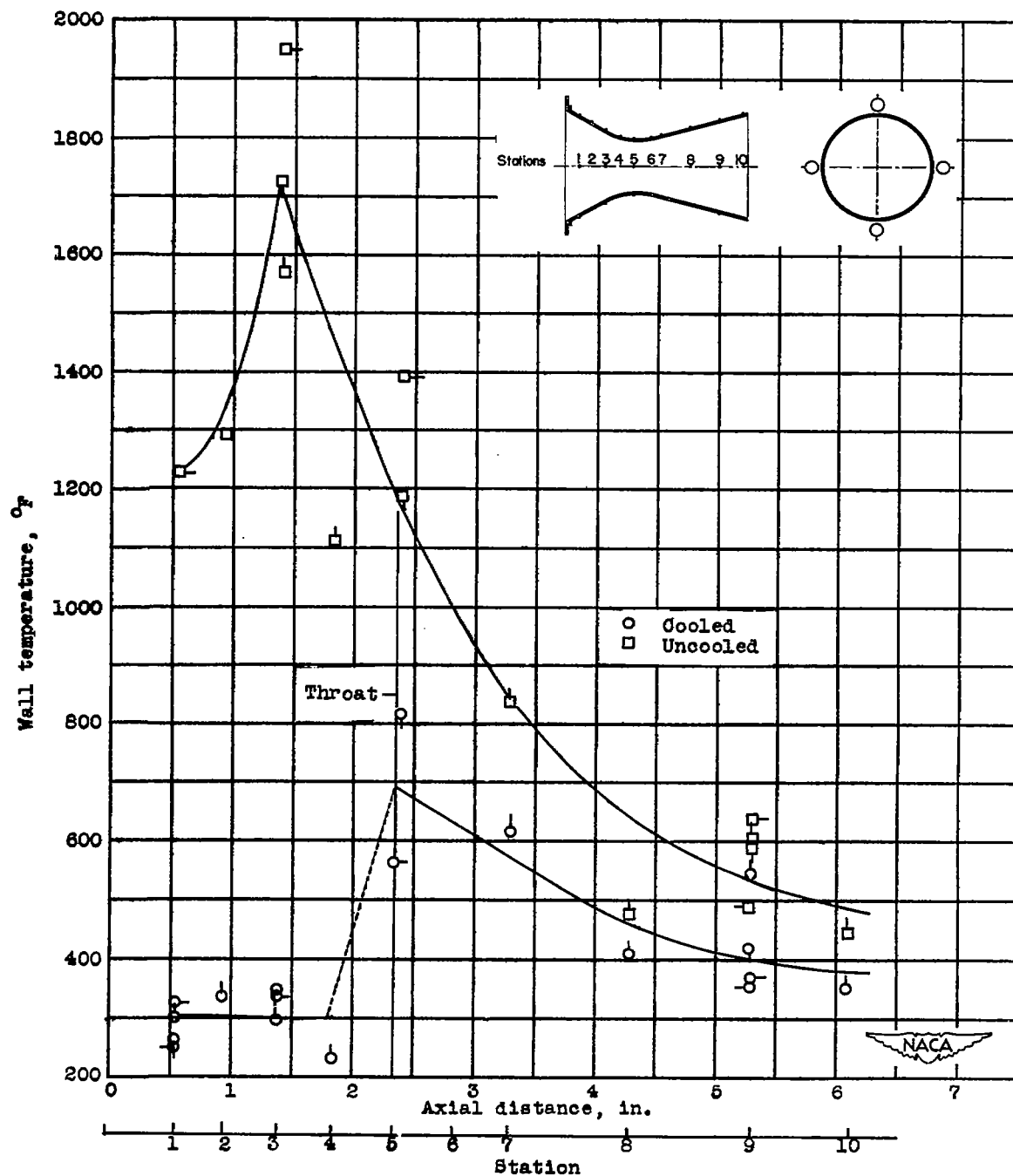
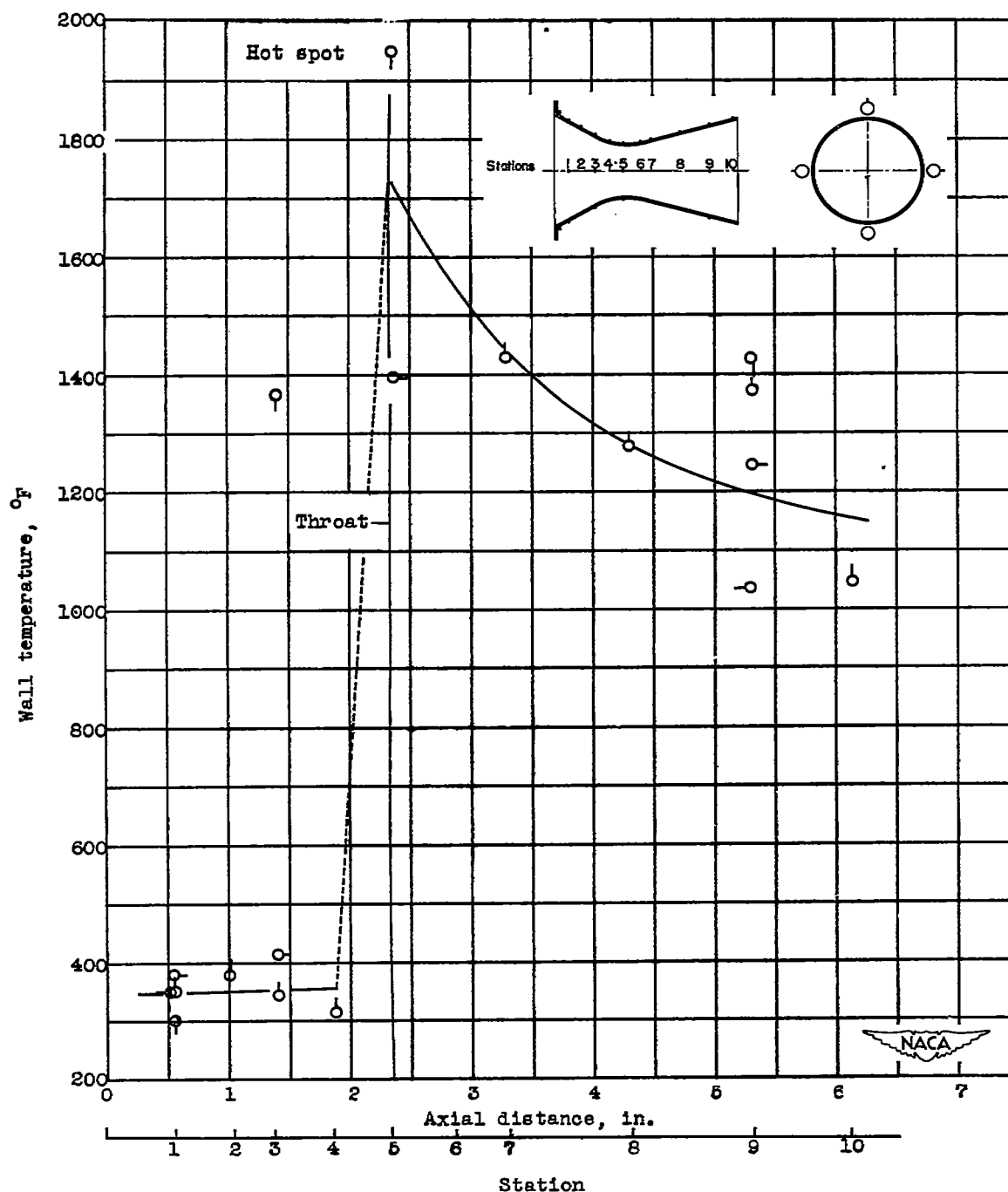


Figure 9. - Effect of water from porous ring at flow of 3.5 percent of propellant flow on wall temperatures of thin-wall stainless-steel nozzle.



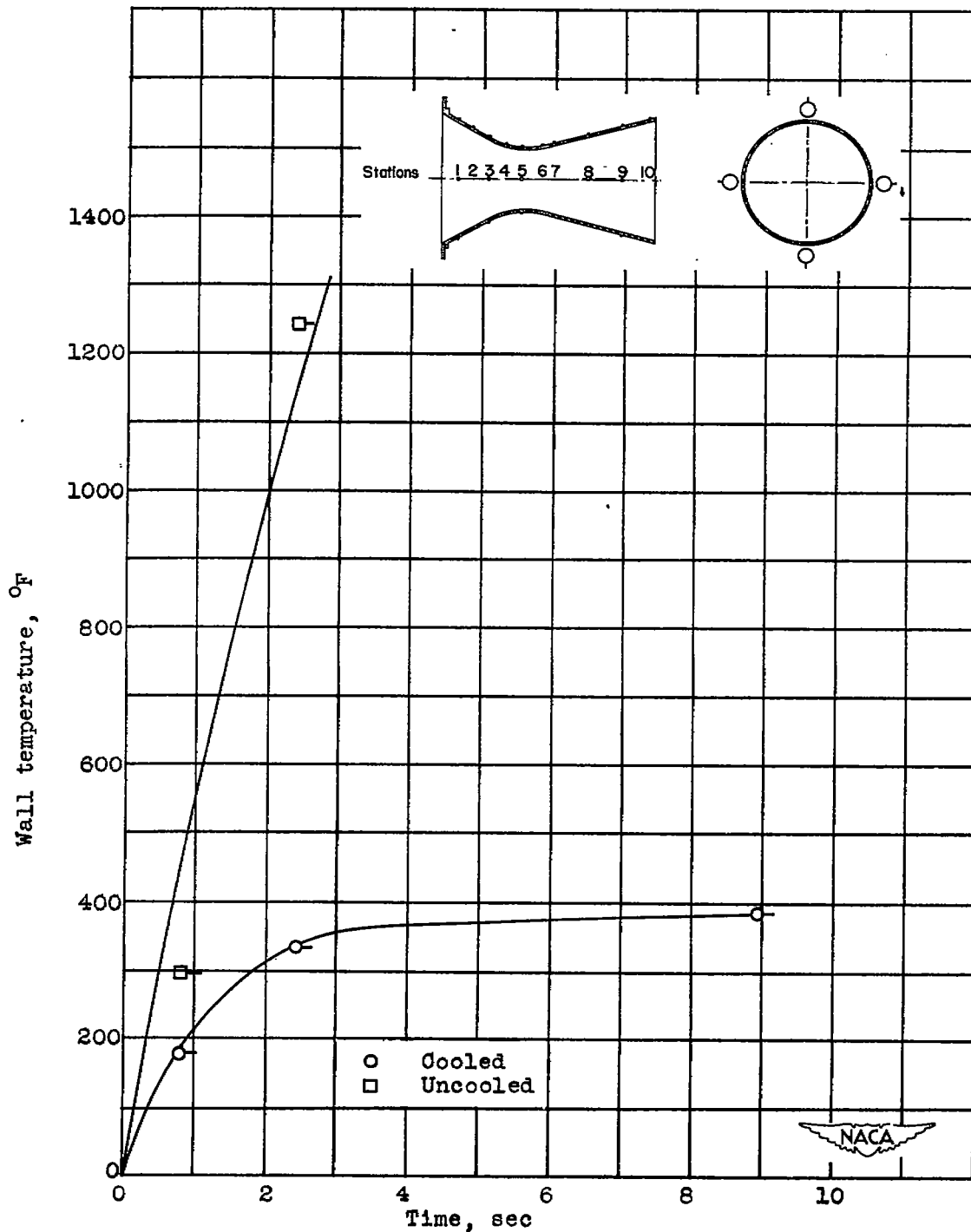
(b) 2.4 seconds.

Figure 9. - Continued. Effect of water from porous ring at flow of 3.5 percent of propellant flow on wall temperatures of thin-wall stainless-steel nozzle.



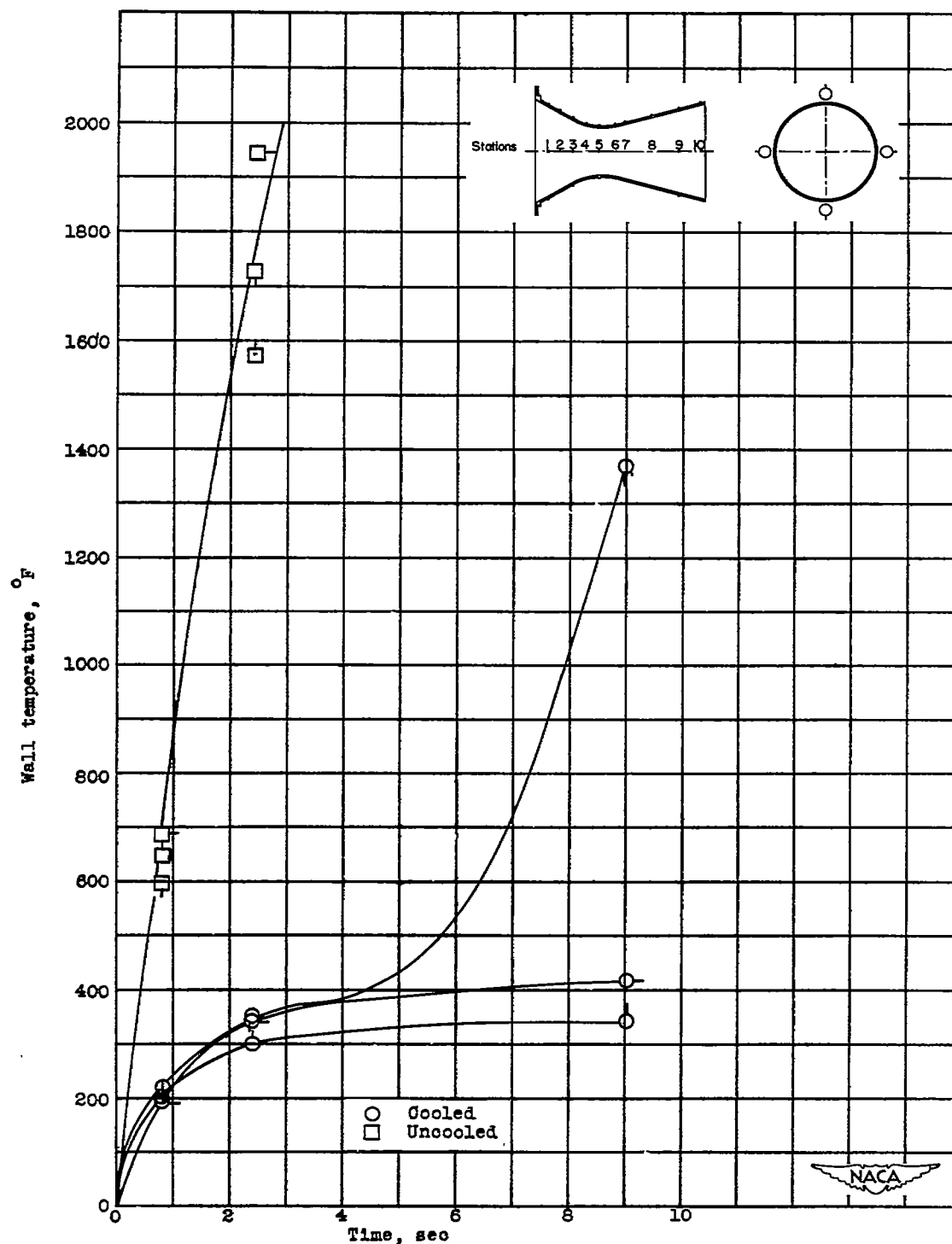
(c) 9 seconds.

Figure 9. - Concluded. Effect of water from porous ring at flow of 3.5 percent of propellant flow on wall temperatures of thin-wall stainless-steel nozzle.



(a) Station 1 (nearest to porous ring).

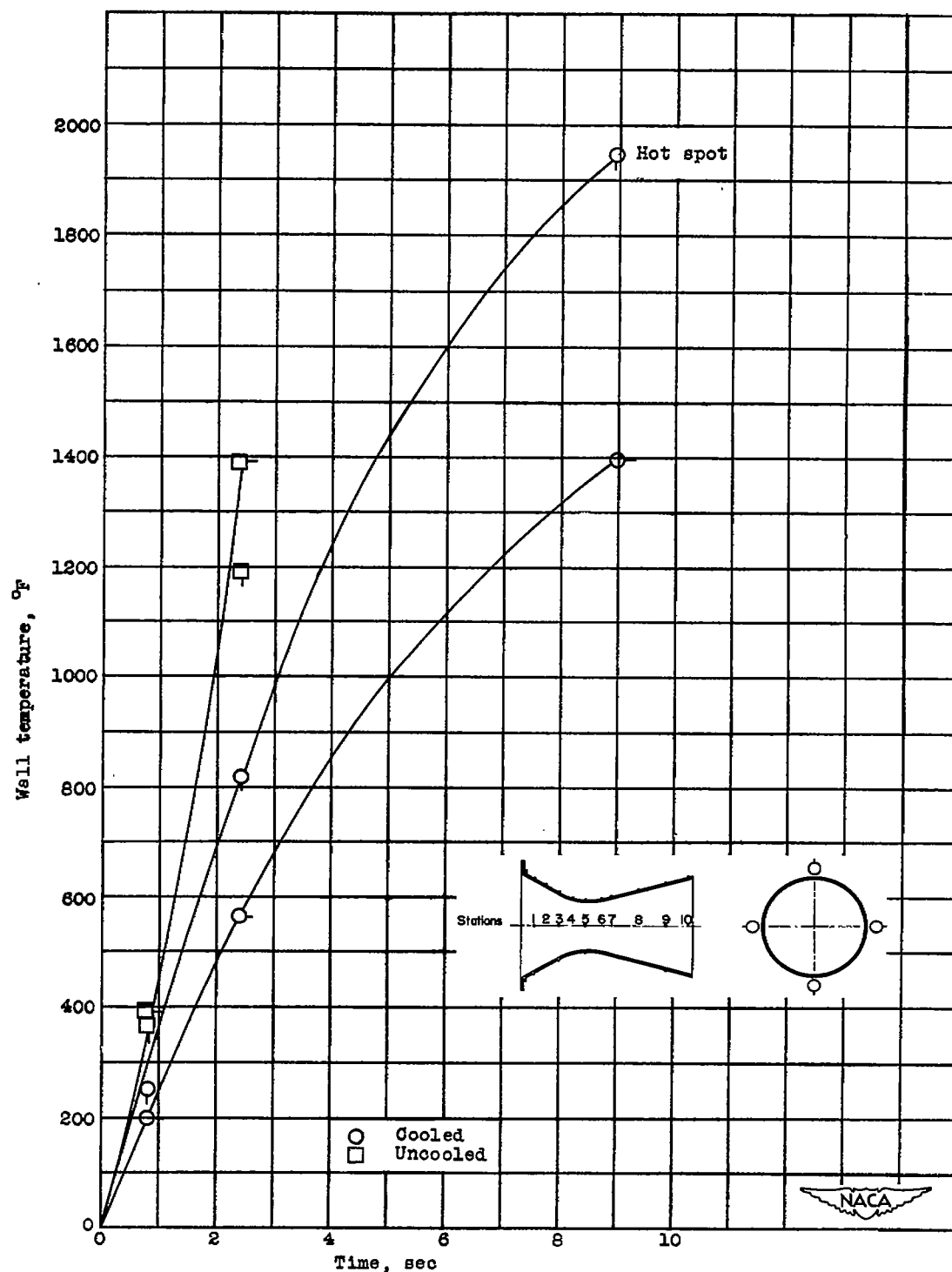
Figure 10. - Wall temperatures of thin-wall stainless-steel nozzles as function of time for uncooled operation and when cooled by water from porous ring at flow of 3.5 percent of propellant flow.



(b) Station 3 (convergent section).

Figure 10. - Continued. Wall temperatures of thin-wall stainless-steel nozzle as function of time for uncooled operation and when cooled by water from porous ring at flow of 3.5 percent of propellant flow.

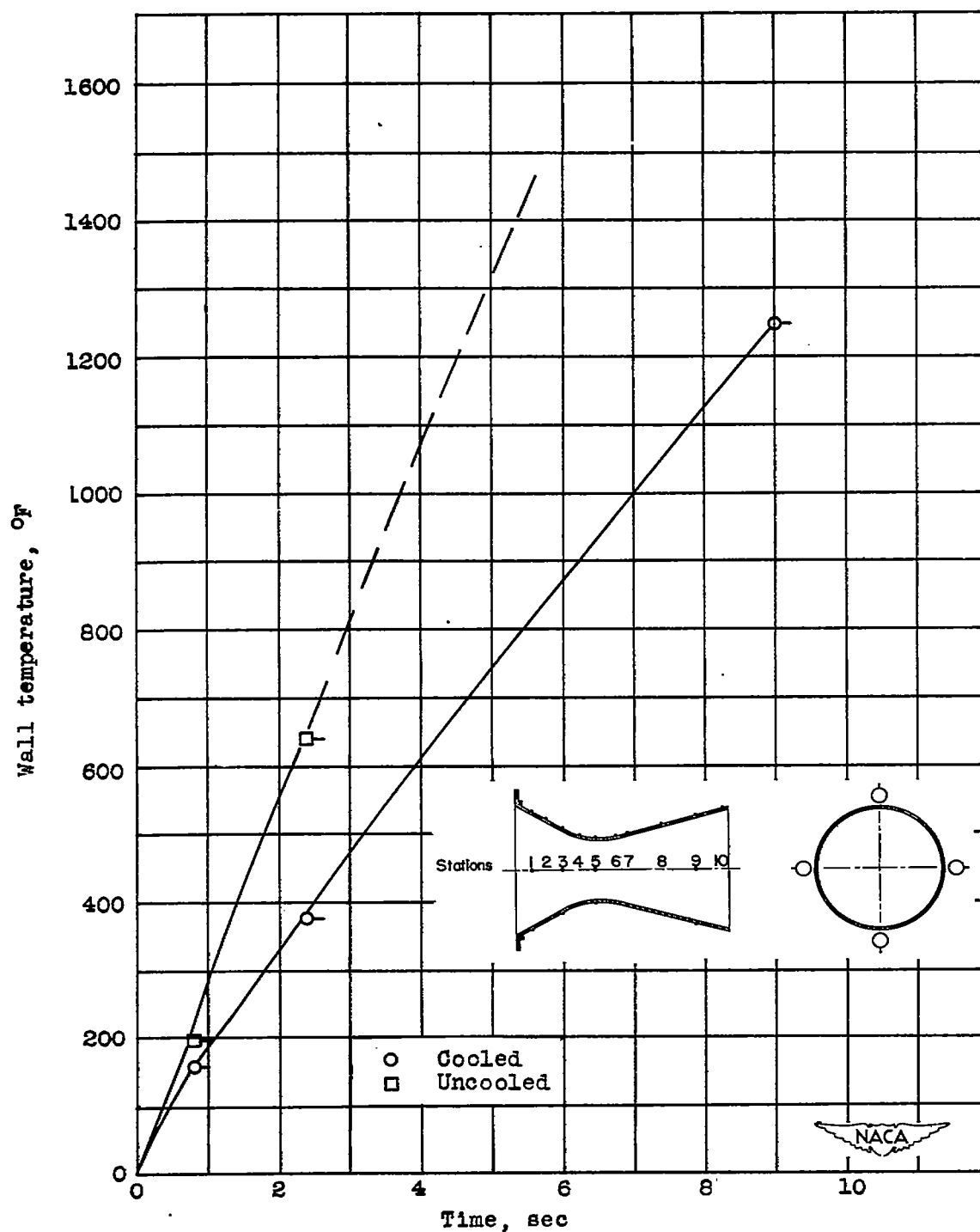
CONFIDENTIAL



(c) Station 5 (throat).

Figure 10. - Continued. Wall temperatures of thin-wall stainless-steel nozzle as function of time for uncooled operation and when cooled by water from porous ring at flow of 3.5 percent of propellant flow.

CONFIDENTIAL



(d) Station 9 (divergent section).

Figure 10. - Concluded. Wall temperatures of thin-wall stainless-steel nozzle as function of time for uncooled operation and when cooled by water from porous ring at flow of 3.5 percent of propellant flow.

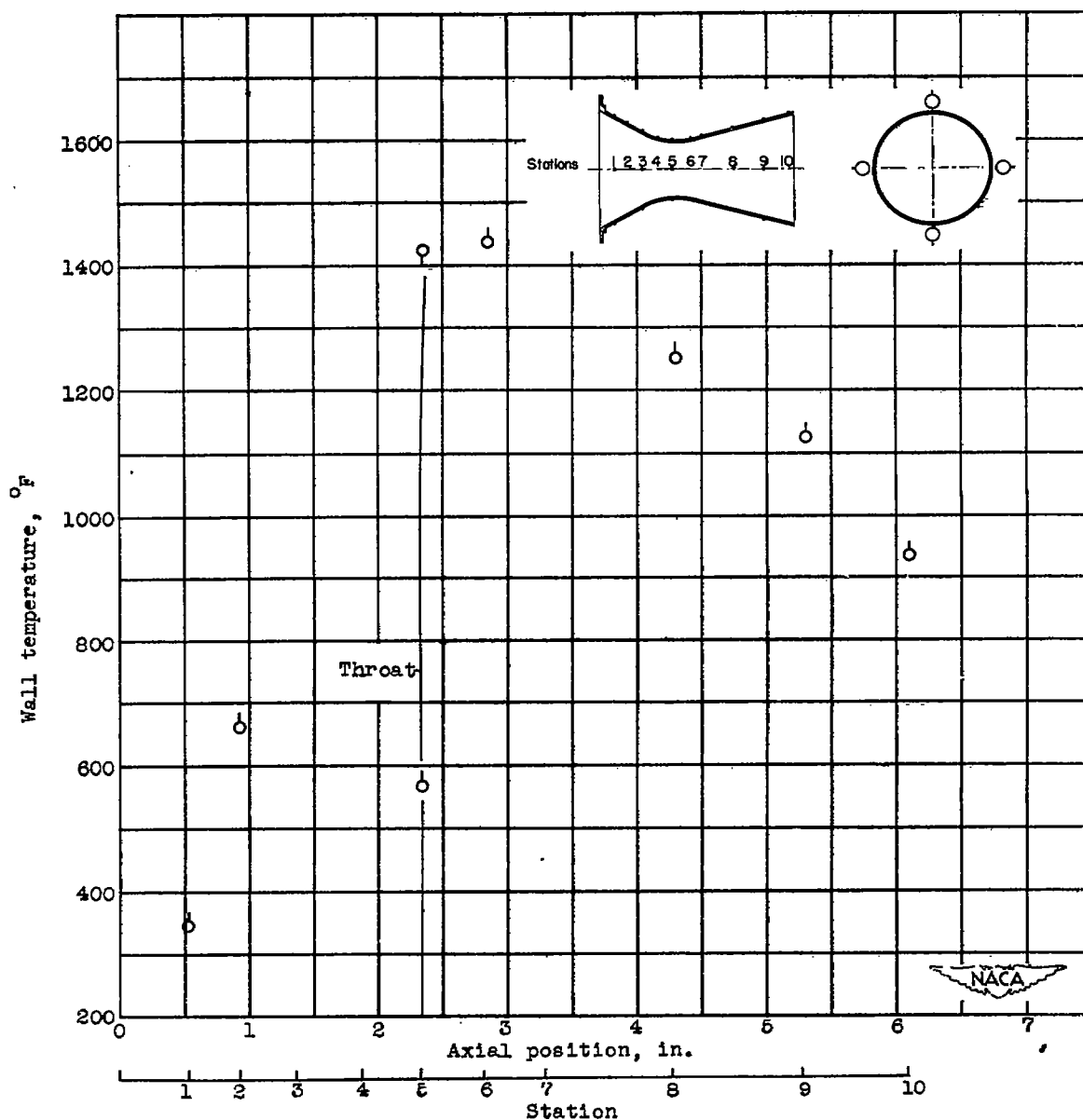


Figure 11. - Wall temperatures of thin-wall stainless-steel nozzle after 9 seconds of operation with jet cooling at water flow of about 8.5 percent of propellant flow.



Figure 12. - Thin-wall stainless-steel nozzle after run with jet cooling along inner surface. Note heat patterns on convergent section.

[REDACTED]

..

.

.

.

.

.

.

.

.

[REDACTED]

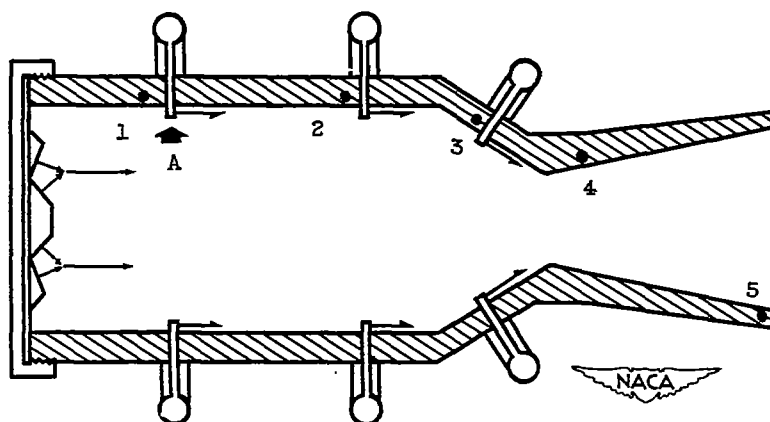
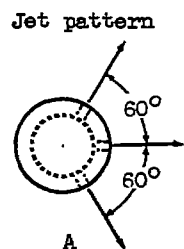
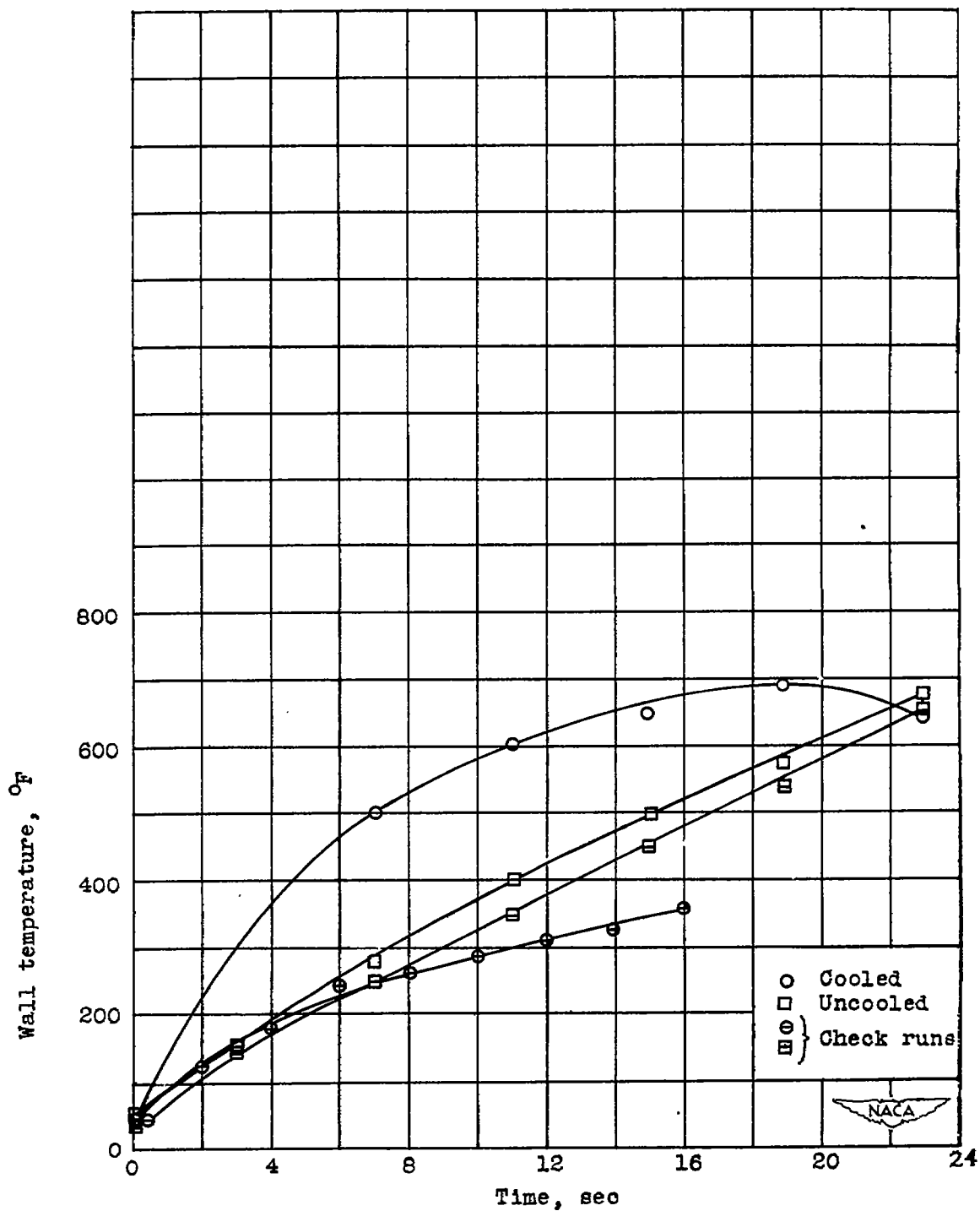
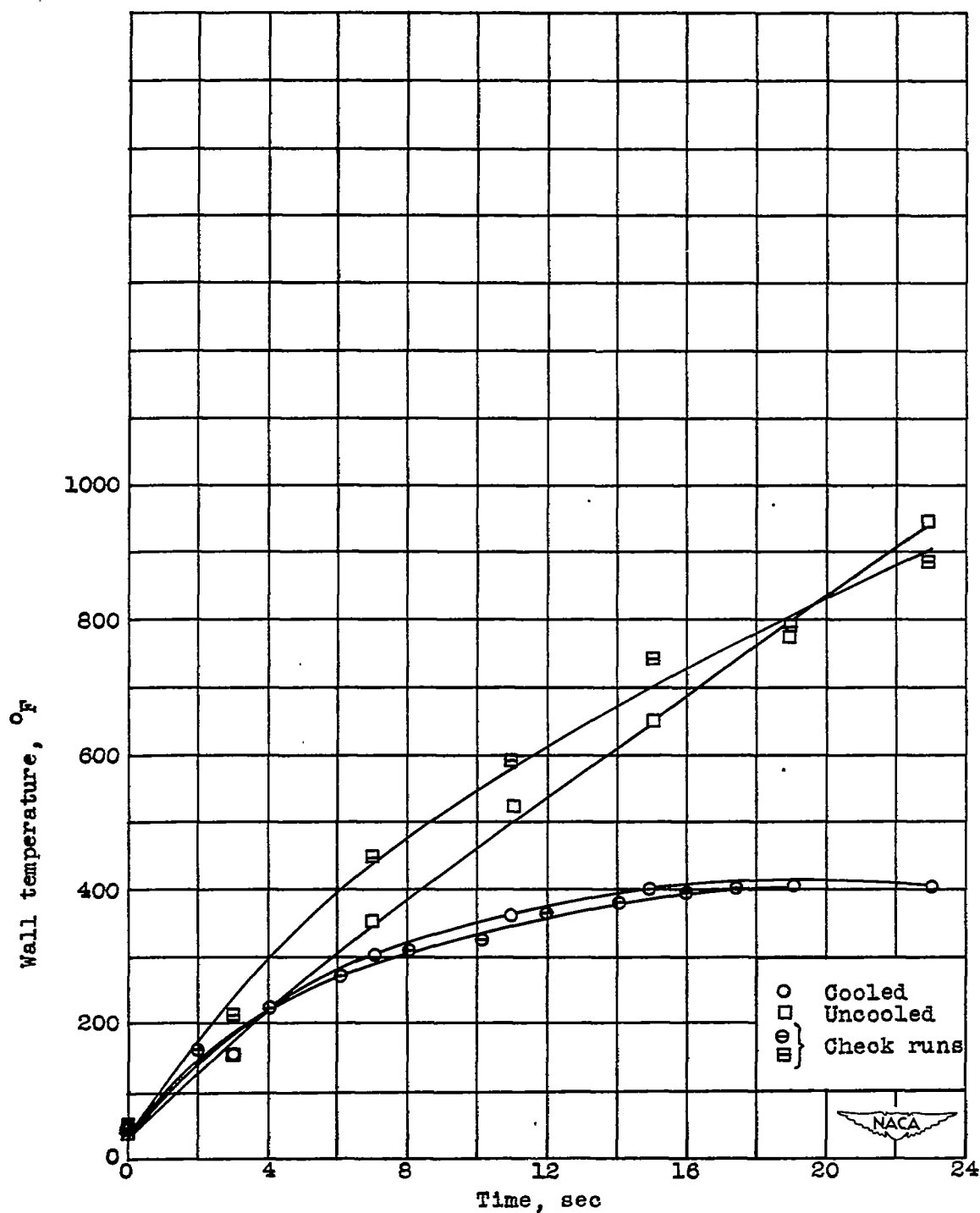


Figure 13. - Diagrammatic sketch of rocket engine cooled by individual jets. Wall thermocouples were located at five positions shown.



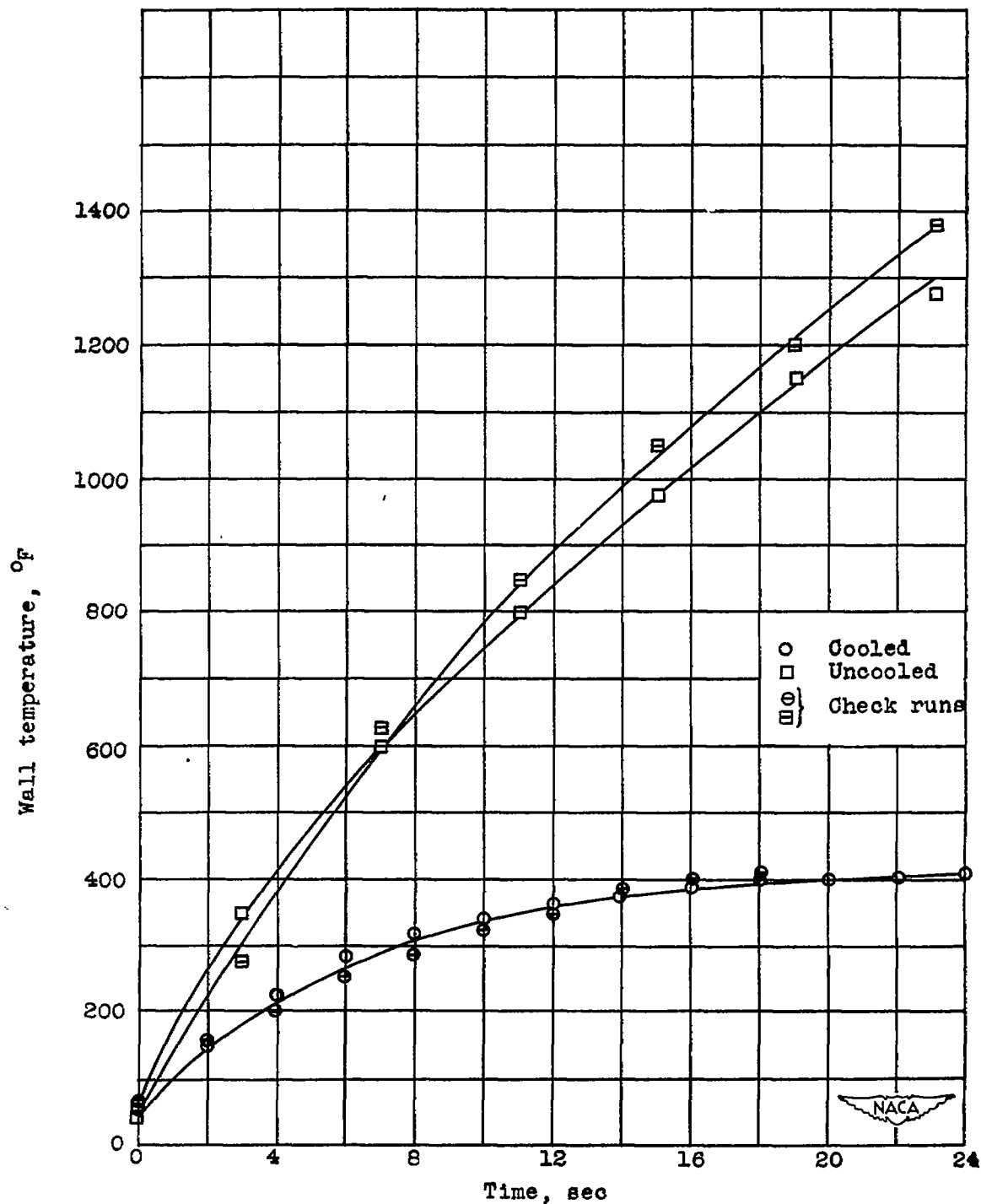
(a) Station 1, behind first injector ring.

Figure 14. - Variation of wall temperature with time in uncooled and in internally film-cooled rocket engine with water flow of approximately 12.5 percent of propellant flow.



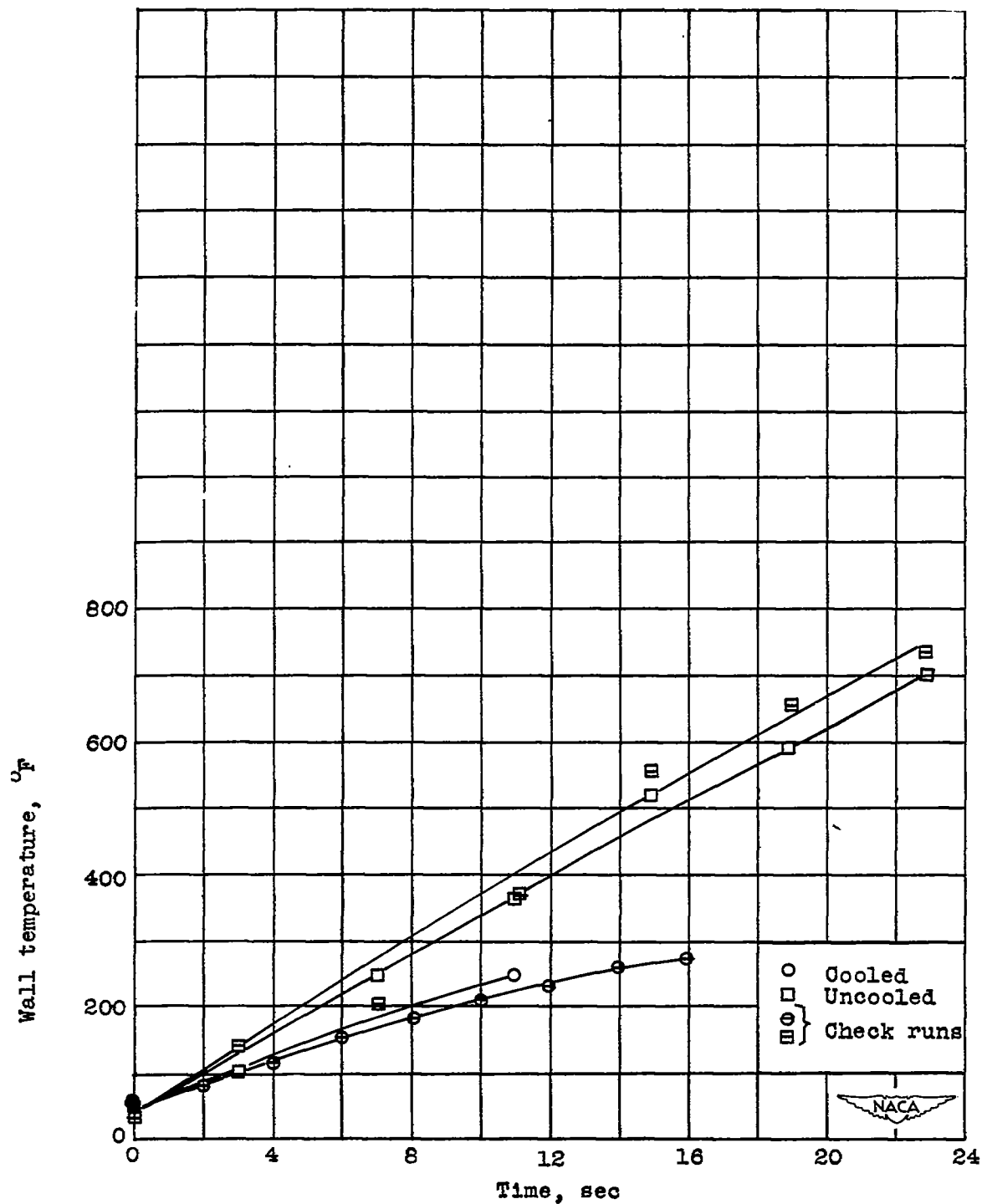
(b) Station 2, behind second injector ring.

Figure 14. - Continued. Variation of wall temperature with time in uncooled and in internally film-cooled rocket engine with water flow of approximately 12.5 percent of propellant flow.



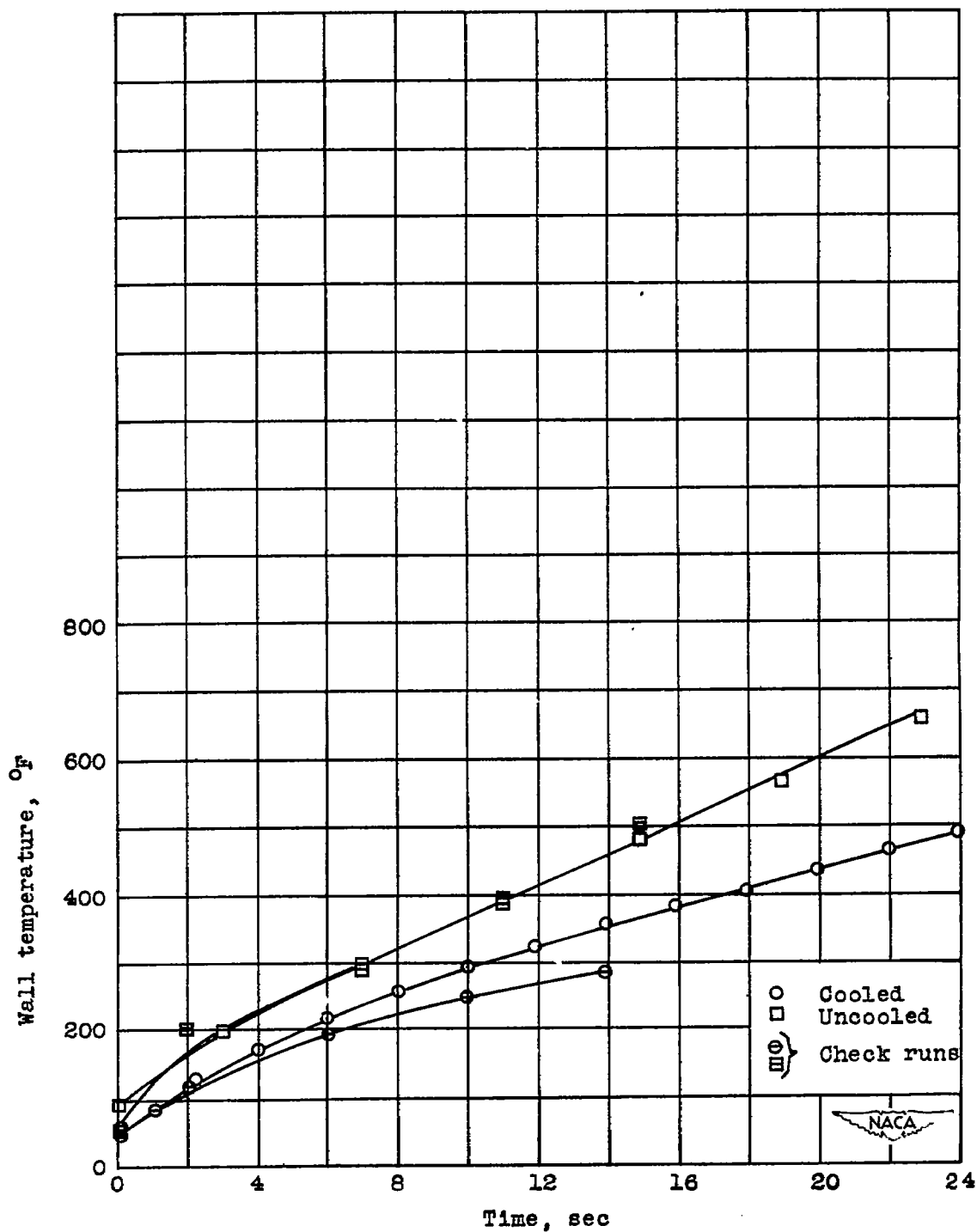
(c) Station 3, convergent section behind third ring of injectors.

Figure 14. - Continued. Variation of wall temperature with time in uncooled and in internally film-cooled rocket engine with water flow of approximately 12.5 percent of propellant flow.



(d) Station 4, throat.

Figure 14. - Continued. Variation of wall temperature with time in uncooled and in internally film-cooled rocket engine with water flow of approximately 12.5 percent of propellant flow.

~~CONFIDENTIAL~~

(e) Station 5, exit.

Figure 14. - Concluded. Variation of wall temperature with time in uncooled and in internally film-cooled rocket engine with water flow of approximately 12.5 percent of propellant flow.

~~CONFIDENTIAL~~